Geoscience Frontiers 10 (2019) 1653–1667

HOSTED BY

Contents lists available at ScienceDirect

China University of Geosciences (Beijing)

Geoscience Frontiers

journal homepage: www.elsevier.com/locate/gsf

Research Paper

Dissolved organic matter tracers reveal contrasting characteristics across high arsenic aquifers in Cambodia: A fluorescence spectroscopy study

Laura A. Richards [a,*], Dan J. Lapworth [b], Daniel Magnone [a,1], Daren C. Gooddy [b], Lee Chambers [c,2], Peter J. Williams [b], Bart E. van Dongen [a], David A. Polya [a]

[a] School of Earth and Environmental Sciences and Williamson Research Centre for Molecular Environmental Science, The University of Manchester, Williamson Building, Oxford Road, Manchester, M13 9PL, UK
[b] British Geological Survey, Maclean Building, Wallingford, Oxfordshire, OX10 8BB, UK
[c] Lancaster Environment Centre, Lancaster University, Lancaster LA1 4YQ, UK

ARTICLE INFO

Article history:
Received 6 October 2017
Received in revised form
23 April 2019
Accepted 26 April 2019
Available online 6 May 2019

Keywords:
Arsenic
Fluorescence spectroscopy
Organic matter characterization
Parallel factor analysis (PARAFAC)
Groundwater quality

ABSTRACT

Organic matter in the environment is involved in many biogeochemical processes, including the mobilization of geogenic trace elements, such as arsenic, into groundwater. In this paper we present the use of fluorescence spectroscopy to characterize the dissolved organic matter (DOM) pool in heavily arsenic-affected groundwaters in Kandal Province, Cambodia. The fluorescence DOM (fDOM) characteristics between contrasting field areas of differing dominant lithologies were compared and linked to other hydrogeochemical parameters, including arsenic and dissolved methane as well as selected sedimentary characteristics. Absorbance-corrected fluorescence indices were used to characterize depth profiles and compare field areas. Groundwater fDOM was generally dominated by terrestrial humic and fulvic-like components, with relatively small contributions from microbially-derived, tryptophan-like components. Groundwater fDOM from sand-dominated sequences typically contained lower tryptophan-like, lower fulvic-like and lower humic-like components, was less bioavailable, and had higher humification index than clay-dominated sequences. Methane concentrations were strongly correlated with fDOM bioavailability as well as with tryptophan-like components, suggesting that groundwater methane in these arsenic-prone aquifers is likely of biogenic origin. A comparison of fDOM tracers with sedimentary OM tracers is consistent with the hypothesis that external, surface-derived contributions to the aqueous DOM pool are an important control on groundwater hydrogeochemistry.

1. Introduction

The structure, composition and abundance of organic matter (OM) in the environment affects many key biogeochemical process, including geogenic arsenic mobilisation in groundwater, a critical public health issue affecting millions of people who are chronically exposed, particularly in South and Southeast Asia (Smedley and Kinniburgh, 2002; Charlet and Polya, 2006; Ravenscroft et al., 2009; World Health Organization, 2011). Environmentally ubiquitous OM is derived from the decay of plant, animal and microbial-sourced organic matter and is highly variable in structure, composition and bioavailability (Hudson et al., 2007). Dissolved organic matter (DOM), operationally defined as the fraction of OM which is < 0.45 μm, is known to have a range of important functions in the aquatic environment as both a source of energy for micro-organisms and in its role in the transport of metals and organic contaminants (McKnight et al., 1992; Benedetti et al., 1996). DOM includes compounds such as chemically well-defined carbohydrates and proteins and less well chemically defined humic substances which include fulvic and humic acids when operationally defined based on their solubility (Thurman, 1985). Several studies show that humic substances are a complex mixture of mainly microbially- and plant-derived biopolymers, with their various breakdown products, and cannot be classed as a distinct

* Corresponding author.
E-mail address: laura.richards@manchester.ac.uk (L.A. Richards).
[1] Present address: School of Geography, University of Lincoln, Brayford Pool, Lincoln, Lincolnshire, LN6 7 TS, UK.
[2] Present address: Department of Civil and Environmental Engineering, University of Strathclyde, Glasgow G1 1XJ, UK.
Peer-review under responsibility of China University of Geosciences (Beijing).

https://doi.org/10.1016/j.gsf.2019.04.009

chemical structure (Kelleher and Simpson, 2006; Lehmann et al., 2008; Kleber and Johnson, 2010; Lehmann and Kleber, 2015). As a result DOM is often a complex mixture of many different compounds and as such is difficult and costly to characterise (Leenheer and Croué, 2003). It is important to distinguish that only certain components of DOM may be labile, or bioavailable, which is defined as the proportion of DOM which is accessible for degradation (Zou et al., 2005), approximately on the timescale of hours to weeks (Davis and Benner, 2007), during microbial processes including microbially-facilitated element cycling. This relative degree of DOM bioavailability thus becomes an important parameter in characterising an overall DOM pool.

Because a significant proportion of OM intrinsically fluoresces (Bech et al., 1993; Hudson et al., 2007), fluorescence spectroscopic techniques have been widely used to characterize the source and composition of DOM in marine waters, freshwaters and wastewater (Coble, 1996; Reynolds and Ahmad, 1997; Baker, 2001; McKnight et al., 2001; Baker and Curry, 2004; Cannavo et al., 2004; Sierra et al., 2005; Holbrook et al., 2006; Hudson et al., 2007). Recent studies have highlighted the use of fluorescence properties to discriminate between different sources of DOM (McKnight et al., 2001; Wilson and Xenopoulos, 2009; Naden et al., 2010; Old et al., 2012) and as a natural tracer to understand groundwater flow processes (Katsuyama and Ohte, 2002; Mariot et al., 2007; Lapworth et al., 2009). Absorption characteristics such as spectral slope can indicate characteristics such as molecular weight (Helms et al., 2008), and fluorescence indices of DOM structure can provide other information on key characteristics of DOM, including the degree of humification, differentiating microbial and terrestrial sources and the degree of structural conjugation and aromaticity (Zsolnay et al., 1999; McKnight et al., 2001).

Excitation/emission matrix (EEM) spectroscopy allows for an overall view of the three-dimensional fluorescence landscape of a particular sample by producing fluorescence spectra at a range of excitation wavelengths. This technique has been applied extensively to characterize dissolved organic matter in natural water for various purposes, including tracing waste water sources and/or leachate (Baker, 2001, 2002; Baker and Curry, 2004; Saadi et al., 2006; Hudson et al., 2007; Huo et al., 2008; Wu et al., 2011, 2012a; Wang et al., 2013; Rhymes et al., 2015), quantification and characterization of marine and/or terrigenic DOM (Mopper and Schultz, 1993; Matthews et al., 1996; Del Castillo et al., 1999; Parlanti et al., 2000; McKnight et al., 2001; Chen et al., 2002, 2003a; Her et al., 2003; Stedmon et al., 2003; Cory and McKnight, 2005; Sierra et al., 2005; Hudson et al., 2007; Murphy et al., 2008; Kowalczuk et al., 2010; Singh et al., 2010a, b; Wu et al., 2012b; Wang et al., 2013; Rhymes et al., 2015; Tye and Lapworth, 2016), tracing groundwater flow and mixing processes (Lapworth et al., 2008, 2009; Rhymes et al., 2015; Tye and Lapworth, 2016), understanding the origin of groundwater methane (Darling and Gooddy, 2006) and characterizing arsenic-affected groundwater (Mladenov et al., 2010, 2015; Kulkarni et al., 2017, 2018a; Vega et al., 2017; Schittich et al., 2018), treated water (Zhang et al., 2008; Wang et al., 2013) and fogwater (Birdwell and Valsaraj, 2010).

EEM is now a routine method, ideal for characterizing fluorescence DOM (fDOM) in natural waters, and has the significant benefit of being rapid ($<\sim$3 min), requires low sample volumes ($<\sim$2 mL) and is non-destructive (Lapworth et al., 2008). EEM allows fDOM components, such as fulvic-like, humic-like and protein-like (tryptophan-like and tyrosine-like) substances, to be identified, which assists with characterizing the fDOM and distinguishing between fDOM sources (Rhymes et al., 2015). For example, the breakdown of plant material is associated with humic-like and fulvic-like substances (Stedmon et al., 2003), whereas readily biodegradable material, such as sewage and farm waste, is associated with high tryptophan-like substances (Baker, 2001, 2002; Naden et al., 2010). High tryptophan-like to fulvic/humic-like ratios, combined with high protein-like fluorescence is characteristic of agricultural diffuse pollution sources (e.g. animal waste) (Baker, 2002; Lapworth et al., 2008). These differing fDOM characteristics allow likely DOM sources to be discriminated within and/or between water bodies (e.g. Lapworth et al., 2009).

Multivariate techniques are commonly used to evaluate and characterize the complex mixtures of fDOM fractions and will be used to analyse EEM data from groundwater samples. One technique for doing this is Parallel Factor Analysis (PARAFAC) (Bro, 1997), which has been widely used for environmental studies (Cory and McKnight, 2005; Hall et al., 2005; Huang et al., 2015). This method essentially decomposes the combined fluorescence signal into individual, distinct modelled components (Bro, 1997; Stedmon et al., 2003; Cory and McKnight, 2005; Lapworth and Kinniburgh, 2009; Kowalczuk et al., 2010; Singh et al., 2010b; Wu et al., 2011; Murphy et al., 2013). PARAFAC models the three-way (excitation, emission, intensity) EEM data using fitting routines to minimise the sum of squares of the residuals (Stedmon and Bro, 2008). The analysis of spectral data is based on the application of Beer-Lambert's law, and there are a number of underlying assumptions that are made including minimal inner filter effects, minimal changes in the local environment (e.g. temperature), and minimal intra-molecular processes. While PARAFAC is often applied to fluorescence data to quantify the overlapping fluorescence components of the EEM (Stedmon et al., 2003; Stedmon and Bro, 2008), the improved utility of this method over carefully chosen subsets of EEM measurements using peak picking techniques is still debated (Murphy et al., 2011).

In the context of arsenic, characterizing DOM is particularly important for understanding the potential role of bioavailable DOM in arsenic mobilization via reductive dissolution of arsenic-bearing iron minerals (Islam et al., 2004). Bioavailable DOM has been postulated to provide electron donors which fuel this microbially-driven reductive dissolution process (Bhattacharya et al., 1997; Islam et al., 2004; Charlet and Polya, 2006; Postma et al., 2007; van Dongen et al., 2008; Rowland et al., 2009). However, the specific nature of DOM implicated in arsenic release and associated controls on arsenic mobilization remain vigorously debated (Nickson et al., 1998; Lawrence et al., 2000; Harvey et al., 2002; McArthur et al., 2004, 2011; Rowland et al., 2007, 2009; Sengupta et al., 2008; van Dongen et al., 2008; Neumann et al., 2009, 2011; Mladenov et al., 2010, 2015; Datta et al., 2011; Sharma et al., 2011; Al Lawati et al., 2012, 2013; Lawson et al., 2013, 2016). Humic substances have been associated with iron-arsenic complexation reactions (Ko et al., 2004; Sharma et al., 2010; Liu et al., 2011; Mikutta and Kretzschmar, 2011), competition for sorption sites with arsenic (Redman et al., 2002; Bauer and Blodau, 2006; Gustaffson, 2006) and electron shuttling (Lovley et al., 1996, 1998, 1999; Nevin and Lovley, 2000; Klapper et al., 2002; Kappler et al., 2004; Jiang and Kappler, 2008; Jiang et al., 2009; Wolf et al., 2009; Mladenov et al., 2010, 2015; Kulkarni et al., 2018b). Methanogenesis has also been demonstrated to be a key influential control on the overall electron flow of DOM degradation, subsequently or correspondingly impacting the rate or extent of the reductive dissolution of iron oxides coupled with arsenic release in reactive transport models (Postma et al., 2016).

In a recent study in an arsenic-affected area in the Bengal Basin, Kulkarni et al. (2017) observed DOM properties to be different in Holocene and Pleistocene aquifers; specifically (i) the Holocene aquifer had a high humification index (HIX), low "freshness index" (β:α), relatively high biological processing of DOM, high ratio of humic-like to protein-like components, high ratio of terrestrially- to microbially-derived components, and higher arsenic and

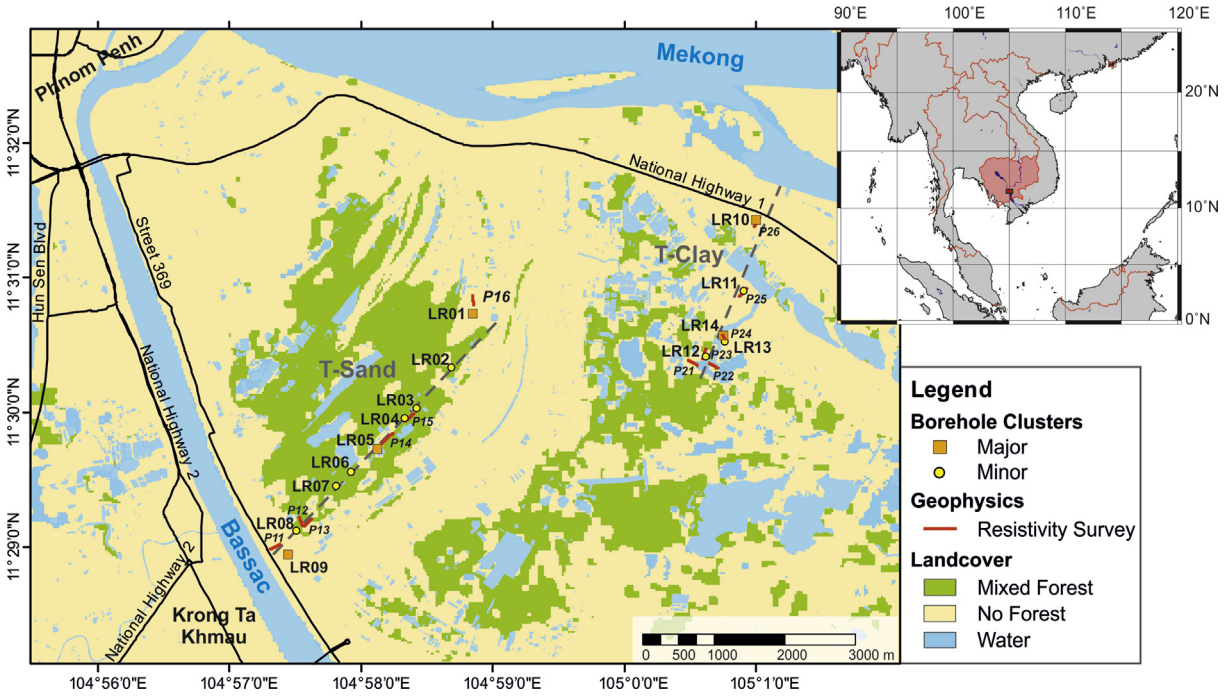

Fig. 1. Field area map (Richards et al., 2017a) in northern Kandal Province, Cambodia, in the lower Mekong basin including field sites (named LR-XX), transects along dominant groundwater flowpaths (T-Sand and T-Clay) and electrical resistivity survey lines (P-XX) (Uhlemann et al., 2017).

reducing conditions, whereas (ii) the Pleistocene aquifer contained more labile DOM sources, a higher proportion of protein-like and microbially-derived components, a relatively lower proportion of biologically-processed DOM, a lower proportion of humic-derived components, with lower arsenic and oxidizing conditions (Kulkarni et al., 2017). This data was used to suggest that the lack of humic-derived DOM in the Pleistocene aquifer may indicate that microbial degradation of DOM did not proceed in the Pleistocene aquifer as it had in the Holocene and may be an important geochemical control on arsenic mobility (Kulkarni et al., 2017). The characteristics of Pleistocene DOM (e.g. high protein-like and low humic-like components) suggest that the Pleistocene DOM would be less likely to participate in interactions such as complexation and competition with arsenic for sorption sites (Kulkarni et al., 2017). In contrast, the more humic Holocene DOM may promote arsenic mobilization (or to maintain arsenic in solution) via the facilitation of reductive dissolution and/or the formation of DOM-arsenic complexes (Kulkarni et al., 2017). It is an interesting question as to whether or not these trends and implications are specific to Bengal aquifers (Kulkarni et al., 2017, 2018a; Vega et al., 2017) or whether they are relevant to other similar arsenic-prone aquifers, for example, well-studied shallow reducing aquifers in Cambodia and elsewhere.

Characterizing the composition of DOM is important for understanding key (bio)geochemical controls on arsenic mobilization and transport in arsenic-affected aquifers. Better understanding of groundwater fDOM, and especially the role of bioavailable DOM, may ultimately assist in improving understanding of arsenic hazards in drinking water and how this may potentially change in the future (Harvey et al., 2002; Polya and Charlet, 2009). The aim of this paper is to characterize and identify the main sources and characteristic nature of DOM in a shallow, reducing arsenic-affected aquifer in northern Kandal Province, Cambodia (Lawson et al., 2013, 2016; Magnone et al., 2017; Richards et al., 2017a, b; Uhlemann et al., 2017) along distinct transects, of differing geochemical characteristics, oriented along dominant groundwater flowpaths. The composition and origins of fDOM in these high resolution profiles have not been studied previously. The objectives were to: (i) characterize the fDOM and distinguish between DOM sources using fluorescence spectroscopy and PARAFAC; and (ii) compare the fDOM pools in contrasting field areas, particularly between sand-dominated and clay-dominated sequences; and (iii) assess the relationship with other sedimentary proxies and aqueous geochemical parameters (including arsenic and methane).

2. Methods and materials

2.1. Field site description

The field area is in the Kien Svay district of northern Kandal Province, Cambodia, an area which is heavily affected by geogenic groundwater arsenic and has been the subject of a number of (ongoing) investigations regarding the (bio)geochemical controls on arsenic mobilization (Polya et al., 2003, 2005; Charlet and Polya, 2006; Tamura et al., 2007; Benner et al., 2008; Kocar et al., 2008; Polizzotto et al., 2008; Rowland et al., 2008; van Dongen et al., 2008; Polya and Charlet, 2009; Lawson et al., 2013, 2016; Magnone et al., 2017; Richards et al., 2017a, b, 2018, 2019a, b). In the current study, field sites are located along two distinct transects, called here “T-Sand” and “T-Clay”, each approximately 3–5 km long, which are dominated by sandy and clay lithologies respectively and are both oriented along inferred major groundwater flowpaths and were initially selected on the basis of electrical resistivity tomography (Uhlemann et al., 2017). Sample IDs are coded in a notation system of LRXX-YY where XX represents the site location and YY is the sample depth (m). A site map (Fig. 1) and schematics of T-Sand and T-Clay transects have been published previously (Richards et al., 2017a).

2.2. Groundwater and surface water sampling and previous characterization

Groundwater (6–45 m depth) and surface water samples were collected from the two transects in 2014 using methods previously described (Richards et al., 2015, 2017a). Data reported in this manuscript are for pre-monsoon samples only; monsoonal differences in geochemistry were typically relatively minor for most sites and details regarding seasonal geochemical and hydrological shifts are reported elsewhere (Richards et al., 2017a). *In-situ* measurements of pH, Eh, dissolved oxygen and electrical conductivity/temperature were made during pumping using a regularly calibrated multimeter (Professional Plus Series Portable Multimeter with sensors 605101, 605102, 605203 and 605301, YSI, UK) using a flow-through cell (603059, YSI, UK). Filtered (0.45 μm syringe filters of regenerated cellulose material housed in polypropylene, Minisart RC, UK) and acidified (pH $<$ 2, trace grade nitric acid, BDH Aristar, UK) water subsamples were analysed for major and trace elements (including arsenic and iron) using inductively coupled plasma atomic emission spectrometer (ICP-AES, PerkinElmer Optima 5300 dual view) and/or inductively coupled plasma mass spectrometry (ICP-MS, Agilent 7500cx) at the University of Manchester (Manchester, UK) (Richards et al., 2017a). Inverse variance weighted first order linear calibration models were used for ICP-AES and ICP-MS (Miller and Miller, 2010; Polya et al., 2017). Filtered and un-acidified water subsamples were analysed for anions (including sulphate) using ion chromatography (IC; Dionex ICS5000 Dual Channel Ion Chromatograph). Dissolved organic carbon (DOC) was measured on subsamples filtered (0.45 μm glass microfiber syringe filters, Whatman/GE Healthcare, UK) and acidified (pH $<$ 2, trace grade nitric acid, BDH Aristar, UK) using a total organic carbon (TOC) analyzer (LABTOC TOC Analyzer, PPM, Netherlands and/or Innovox Lab TOC Analyzer, GE, UK, depending on analytical batch). Samples collected for cation, anion and DOC analysis were stored in 100 mL glass Schott bottles which were acid-washed and furnaced before use. Further method details regarding inorganic characterization, including quality assurance/quality control measures, are provided elsewhere (Polya et al., 2017; Richards et al., 2017a).

The methods for sedimentary C:N and lipid analysis (including sedimentary sampling techniques) are detailed elsewhere (Magnone et al., 2017); in brief, total sedimentary C and N were measured using an elemental analyser (Vario El Cube, Elementar) at the University of Manchester and validated by an external laboratory (Elemental Lab, Okehampton, Devon, UK). Lipid biomarkers were extracted and analysed using gas chromatography mass spectrometry (Agilent 789A GC and Agilent 5975C MSD) at the University of Manchester using separation techniques previously published (Rowland et al., 2006; van Dongen et al., 2006, 2008; Al Lawati et al., 2012).

2.3. Fluorescence measurements

Subsamples for fluorescence analysis were filtered in the field (0.45 μm cellulose and polypropylene syringe filters, Minisart RC, UK) and stored in glass bottles, un-acidified, in the dark at approximately 4 °C prior to analysis (subsamples were the same as used for anion analysis). Un-acidified samples were used for representation of environmental conditions; in a separate study, acidification has been demonstrated to affect various fDOM optical properties (Kulkarni et al., 2019). A Varian™ Cary Eclipse fluorescence spectrometer was used for the fluorescence analysis. Excitation (Ex) wavelengths were set between 200 and 400 nm with a 5 nm bandwidth and emission (Em) wavelength were set between 250 and 500 nm with a 2 nm bandwidth. The photomultiplier tube (PMT) voltage was set to 725 V, and all analysis was carried out in quartz vials with a path length of 1 cm. All fluorescence results are reported as an average of three repeat analyses, following blank subtraction, and are presented in Raman Units (RU), normalised to the area under the water Raman peak of ultrapure water blanks at Ex 350 nm–Em 397 nm. Ultraviolet absorbance measurements at 254 nm (Abs_{254}) were carried out using a Varian (UV/visible) spectrophotometer with a cell path of 1 cm. The specific ultraviolet absorbance (SUVA) is the ratio of Abs_{254} and the DOC concentration (Chen et al., 2003b). Ultrapure water (ASTM type I reagent grade water, including a UV cracker) was used for blank samples and to clean the quartz cell between samples. Several samples ($n = 3$) were evaluated for time-series stability to estimate the impact of sample storage time on fluorescence results. All fluorescence measurements were made at the British Geological Survey (Wallingford, UK).

Following absorbance correction, using the method of Lakowicz (1991), and blank correction a number of fluorescence indices were calculated using standard peak picking techniques which have been shown to relate to DOM structure and source: (i) the fluorescence index (FI) which is commonly used to differentiate between terrestrial and microbial DOM sources (McKnight et al., 2001); (ii) the humification index (HIX), an indication of humicity, and the condensing of fluorescing molecules (Zsolnay et al., 1999); (iii) the humification index corrected for inner-filtering (HIX_{corr}) (Ohno, 2002); (iv) the xenobiotic organic matter (XOM) index as defined by Ex: 220–230 nm and Em: 340–370 nm (Baker and Curry, 2004) which is a proxy for polycyclic aromatic hydrocarbon (PAH) compounds with typically two or three rings (e.g. naphthalene) which could be anthropogenically or naturally produced (depending on setting/depth); (v) the "freshness index" β:α, relating to the relative amounts of labile DOM (β, often microbially produced or autochthonus/*in-situ*) to recalcitrant terrestrial carbon (α, allochthonous) (Parlanti et al., 2000; Wilson and Xenopoulos, 2009; Kulkarni et al., 2017), noting that higher molecular weight humic-like DOM sorbs preferentially to goethite (α-FeOOH) as compared to lower molecular weight DOM (Ohno et al., 2007); (vi) humic-like fluorescence (HA-like) (Chen et al., 2003b); (vii) fulvic-like fluorescence (FA-like); (viii) tryprophan-like fluorescence (TPH-like) and (ix) the ratio of two fluorescing components (TPH:FA), one representing more recent labile DOM, and one representing recalcitrant DOM (Parlanti et al., 2000; Wilson and Xenopoulos, 2009). TPH:FA (which explicitly includes a TPH-like component and the FA-like component) differs in definition from β:α, a proxy for autochthonous microbially-derived DOM, which describes humic-like components of varying expected bioavailability (β defined as Ex_{max}: 310–320 nm and Em_{max}: 380–420; α defined as Ex_{max}: 330–350 nm and Em_{max}: 420–480 nm) (Parlanti et al., 2000). Data was processed and indices were calculated using R software (Lapworth and Kinniburgh, 2009; R Core Team, 2015).

2.4. Parallel factor analysis (PARAFAC)

Parallel factor analysis (PARAFAC) was undertaken on absorbance and blank corrected EEMs to extract, model and quantify the spectrally overlapping fluorescence components of each EEM. PARAFAC uses a least-squares algorithm to decompose the data, for further details on the method and approach see Stedmon et al. (2003). The 'DOMFluor v1.7' toolbox (Stedmon and Bro, 2008) was used to undertake this analysis, explore the data set and validate the PARAFAC modelling. Rapid model convergence was obtained and validated using independent split-half analysis of the data set following removal of outlier data which had high leverage (Stedmon and Bro, 2008). A three component model was able to satisfactorily model the EEM domain in the data set and components (i.e. F_{max}) were reported in RU. Total fluorescence (TF, in RU) was calculated as the sum of the three PARAFAC components.

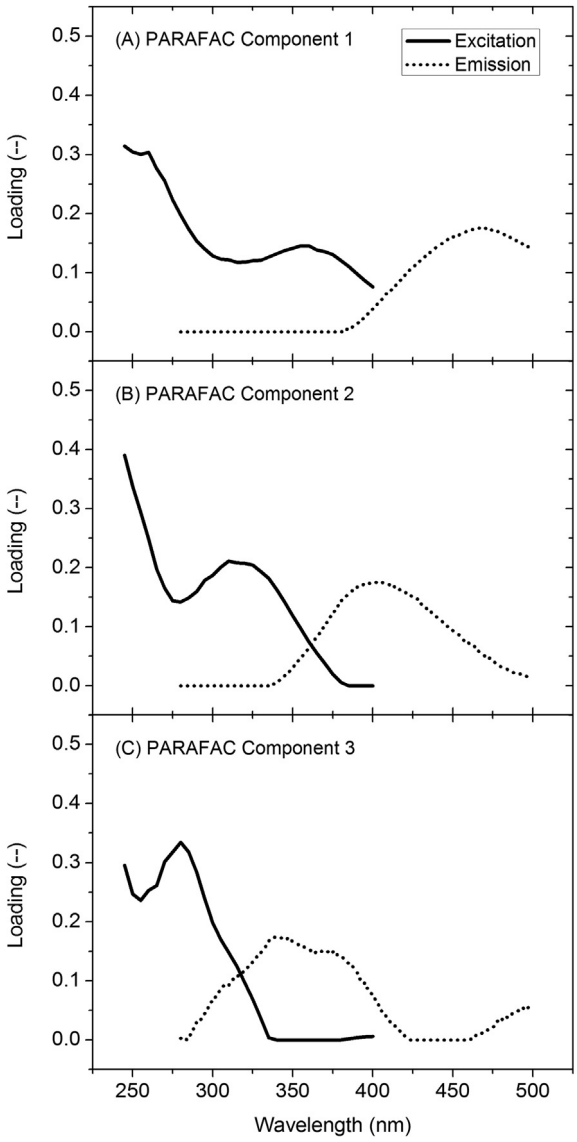

Fig. 2. Excitation and emission loading for modelled PARAFAC components humic-like C1, humic-like C2 and tryptophan-like C3 (A, B, C, respectively).

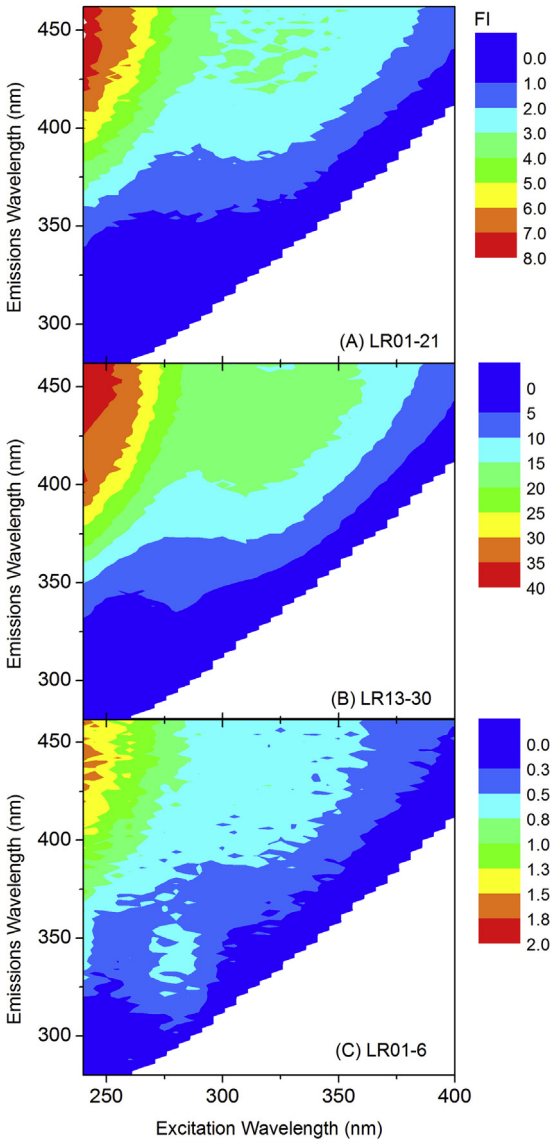

Fig. 3. Representative EEM spectra showing absorbance-corrected fluorescence intensity (FI) (Parker and Barnes, 1957) for groundwater at (A) LR01-21 with comparatively high proportional humic-like C1; (B) LR13-30 with comparatively high proportional humic-like C2; and (C) LR01-6 with comparatively high proportional tryptophan-like C3. Note differences in fluorescence intensity scales.

2.5. Methane analysis

Samples for methane (CH_4) and ethane (C_2H_6) analysis were collected into double-valve steel cylinders of known capacity (mean volume 50.9 cm^3, range 47–55 cm^3). Samples for methane analysis were collected from selected groundwater monitoring wells in December 2015 after the completion of the major 2014 groundwater sampling campaigns; seasonal differences in groundwater geochemistry are expected to be small compared to differences with sample locality and depth (Richards et al., 2017a). All sample processing and analysis was carried out in the laboratories at BGS Wallingford using methods previously reported (Gooddy and Darling, 2005; Darling and Gooddy, 2006; Bell et al., 2017). In brief, a headspace technique was used to transfer the water and gas in the sampling cylinder to an evacuated glass bulb of known capacity (mean volume 121.1 cm^3, range 117–123 cm^3) using helium as a displacing gas. Aliquots of the headspace gas were expanded into the evacuated inlet system of the Gas Chromatograph (GC), from where they were admitted to a 1/8th-inch (3.2 mm) outer diameter Porapak-Q packed column at room temperature. Eluting methane was detected by a flame ionisation detector (FID). The detection limits for dissolved methane and ethane were approximately 0.5 μg L^{-1} and 2.5 μg L^{-1}, respectively. Canned gas standards (Air Products Ltd.) covering the decades from 1×10^5 μg L^{-1} to 1×10^8 μg L^{-1} methane were used for calibration which is linear over this range. Measurement precision is estimated to be around ±5% RSD for most of the samples analysed.

3. Results and discussion

3.1. PARAFAC components

Three components were defined in PARAFAC modelling (Fig. 2): (i) Component 1 (C1), characterized by peak fluorescence at higher Em (~470 nm) and Ex (245 and 360 nm); (ii) Component 2 (C2), characterized by maxima at mid-Em (~400 nm) and Ex (245 and 310 nm); and (iii) Component 3 (C3), characterized by maxima at

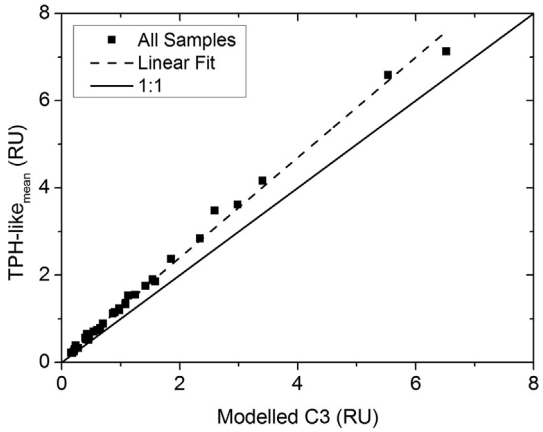

Fig. 4. Tryptophan-like, absorbance-corrected fluorescence peak identified by mean peak picking (TPH-like$_{mean}$) versus modelled PARAFAC component C3.

lower Em (~340 nm) and Ex (~280 nm). The components identified here are broadly similar to those identified in other studies of aquatic environments (Parlanti et al., 2000; Chen et al., 2003b; Stedmon et al., 2003; Kulkarni et al., 2017). C1 and C2 are consistent with humic-like components and likely to be derived from terrestrial OM, and C3 is consistent with tryptophan-like OM and likely to be derived from microbial/protein-based components (Chen et al., 2003b; Kulkarni et al., 2017). Representative EEM spectra for selected groundwater samples (Fig. 3) show the fluorescence matrix for samples with relatively high values for C1, C2 and C3. The absorbance-corrected fluorescence intensities are sample and component specific, with the tryptophan-like C3 proportionally much smaller than the humic-like C1 and C2 fractions in most samples, as would be expected for typical groundwaters (e.g. Lapworth et al., 2009; Huang et al., 2015). The PARAFAC fluorescence peak for trytophan-like C3 is strongly correlated with the absorbance-corrected, mean tryptophan-like fluorescence peak identified by peak picking (t (33) = 75.0, $p < 0.05$) (Fig. 4), with the peak-picking method overestimating the PARAFAC obtained value by ~15%.

3.2. Time series stability and impact of sample agitation

A selected number of samples ($n = 3$) was evaluated for stability during storage, particularly given the time (approximately 2 years) that passed between the original collection of samples and EEM analysis due to logistical constraints (noting that samples were stored appropriately during that time). Time series data (Fig. 5) over approximately 7 months of storage shows no significant or

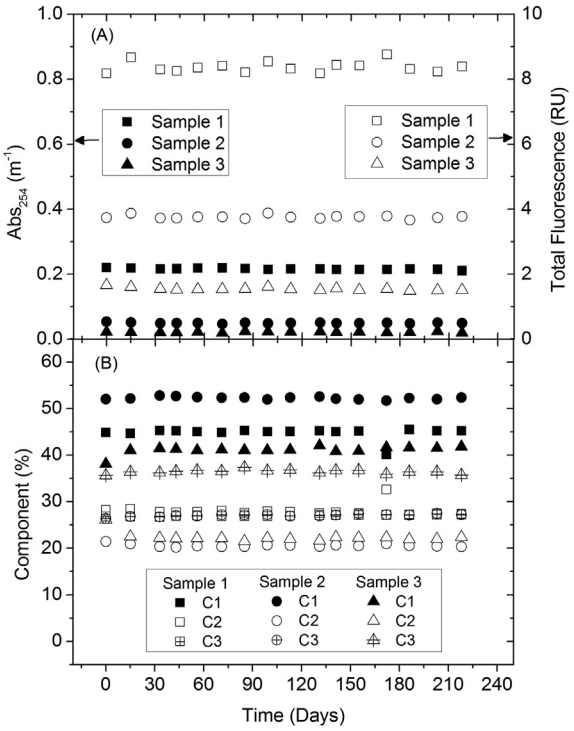

Fig. 5. EEM data from samples stored over approximately 7 months for 3 representative samples of differing characteristics for (A) absorbance at 254 nm (m^{-1}) (Abs$_{254}$) and calculated total fluorescence (as C1 + C2 + C3, all in RU) and (B) modelled PARAFAC components C1, C2 and C3 as a proportion of total composition.

systematic change in either absorbance or composition as modelled by PARAFAC components. The samples shown in Fig. 5 were collected from a nearby study site specifically for the purpose of evaluating the stability of measured EEM data during storage and are not otherwise included in this manuscript. Even though the samples are of slightly different origin, a similar degree of stability over time is expected for the other samples reported in this manuscript.

Further, in a limited number of cases ($n = 2$), PARAFAC models did not reach convergence or pass validation tests and these samples were therefore excluded from the dataset. This lack of convergence is attributed to scattering artefacts typically due to iron hydroxide precipitates. A comparison was made in order to evaluate any impact on the results from gently shaking samples immediately before analysis versus leaving samples undisturbed (and thus not agitating any settled precipitates) (Fig. 6). A

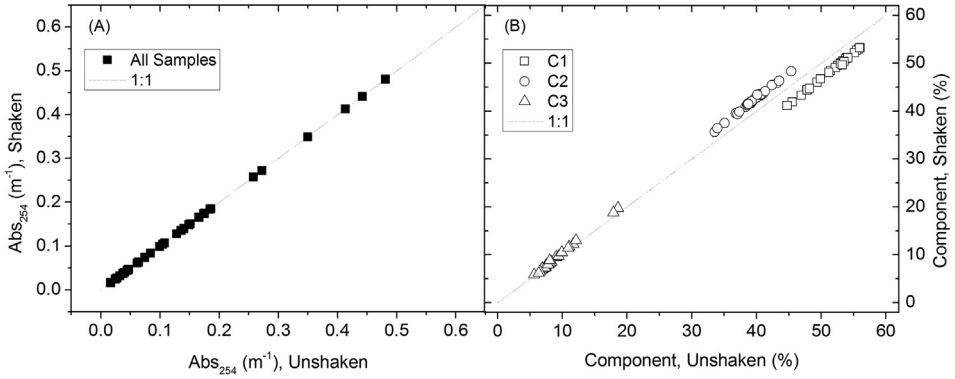

Fig. 6. Comparison of analysis of samples that were shaken directly before analysis versus those that were unshaken for (A) absorbance (m^{-1}) at 254 nm and (B) modelled PARAFAC components C1, C2 and C3.

Table 1
Chemical and fDOM characteristics of groundwater (GW) from T-Sand and T-Clay and surface waters (SW) in northern Kandal Province, Cambodia. Values are reported as mean (minimum–maximum).

	T-Sand, GW; Mean (range) ($n = 23$)	T-Clay, GW; Mean (range) ($n = 11$)	SW; Mean (range) ($n = 3$)	p-value; Mann-Whitney GW Comparison[h]
Water geochemistry[a]				
As ($\mu g\ L^{-1}$)	324 (11–835)	315 (2–1092)	4 (2–8)	>0.05 (0.82)
Fe ($mg\ L^{-1}$)	7.6 (0.0–26.9)	3.8 (0.1–11.6)	0.1 (0.0–0.3)	>0.05 (0.06)
SO_4^{2-} ($mg\ L^{-1}$)	5.1 (<1–15.5)	65.4 (<1–326)	13.1 (2.1–19.0)	>0.05 (0.15)
DOC ($mg\ L^{-1}$)	3.4 (0.8–7.9)	7.3 (1.5–18.0)	5.0 (1.5–12.0)	<0.05 (0.03)
Eh (mV)	−121 (−176–8)	−93 (−178–28)	32 (−205–169)	>0.05 (0.22)
Absorbance				
Abs_{254} (m^{-1})	0.10 (0.02–0.26)	0.21 (0.03–0.48)	0.14 (0.03–0.35)	>0.05 (0.11)
SUVA ($L\ mg^{-1}\ m^{-1}$)	0.031 (0.000–0.128)	0.026 (0.016–0.044)	0.026 (0.025–0.029)	n/a
TPH-$like_{mean}$ (RU)	1.16 (0.22–3.49)	3.28 (0.33–8.99)	1.10 (0.39–2.38)	>0.05 (0.08)
TPH-$like_{max}$ (RU)	1.47 (0.26–4.40)	4.08 (0.37–11.3)	1.40 (0.46–3.12)	>0.05 (0.11)
FA-$like_{mean}$ (RU)	3.37 (0.53–11.2)	8.18 (0.97–19.9)	3.10 (0.60–7.72)	>0.05 (0.13)
FA-$like_{max}$ (RU)	3.72 (0.58–12.3)	8.59 (1.06–20.6)	3.32 (0.74–8.11)	>0.05 (0.14)
HA-$like_{mean}$ (RU)	2.77 (0.35–8.88)	6.30 (0.71–15.5)	2.29 (0.42–5.82)	>0.05 (0.16)
HA-$like_{max}$ (RU)	2.97 (0.39–9.38)	6.63 (0.78–16.2)	2.47 (0.47–6.2)	>0.05 (0.18)
Fluorescence indices				
FI[b]	1.30 (0.93–1.84)	1.34 (1.06–1.67)	1.48 (1.21–1.71)	>0.05 (0.31)
TPH:FA	0.37 (0.27–0.92)	0.41 (0.30–0.52)	0.53 (0.31–0.88)	<0.05 (0.03)
HIX[c]	14.7 (5.53–19.3)	12.2 (7.30–18.8)	12.2 (5.96–20.0)	≈0.05 (0.05)
HIX_{corr}[d]	0.93 (0.85–0.95)	0.92 (0.88–0.95)	0.91 (0.86–0.95)	≈0.05 (0.05)
XOM[e]	0.25 (0.05–0.60)	0.60 (0.07–1.51)	0.19 (0.07–0.41)	>0.05 (0.16)
β:α	0.59 (0.53–0.77)	0.67 (0.52–0.78)	0.52 (0.46–0.57)	<0.05 (0.02)
PARAFAC (RU)				
C1	6.12 (0.82–20.0)	12.1 (1.79–32.8)	6.11 (1.16–15.6)	>0.05 (0.25)
C2	4.42 (0.74–15.1)	10.2 (1.37–28.4)	4.55 (0.82–11.7)	>0.05 (0.20)
C3	0.88 (0.16–2.59)	2.28 (0.27–6.52)	0.84 (0.23–1.85)	>0.05 (0.14)
Calculated parameters				
TF[f] (RU)	11.4 (1.7–37.8)	24.6 (3.5–67.7)	11.5 (2.4– 9.2)	n/a
C1 (%)	53.2 (47.8–56.0)	49.3 (44.7–54.1)	51.7 (48.2–53.5)	n/a
C2 (%)	38.6 (33.5–43.2)	41.5 (38.6–45.4)	37.6 (33.9–40.1)	n/a
C3 (%)	8.2 (5.6–18.6)	9.3 (6.5–12.1)	10.8 (6.3–17.9)	n/a
HA:TPH[g]	11.9 (4.4–16.7)	10.2 (7.3–14.4)	10.3 (4.6–14.8)	n/a

[a] Values calculated for this dataset from Richards et al. (2017a).
[b] Fluorescence index (FI) as given in McKnight et al. (2001).
[c] Humification index (HIX).
[d] HIX with inner-filtering correction (Ohno, 2002).
[e] Xenobiotic organic matter (XOM) index (Baker and Curry, 2004).
[f] Total fluorescence (TF) calculated as C1 + C2 + C3 (in RU).
[g] Calculated as (C1 + C2)/C3 (in RU).
[h] p-values calculated by the Mann-Whitney Test using OriginPro 8.5.1 for non-parametric statistics to compare the T-Sand and T-Clay GW sample distributions; p-values < 0.05 indicate that the sample distributions are significantly different at the 95% confidence level; n/a is not applicable as parameters calculated from datasets already statistically compared.

comparison of both Abs_{254} (Fig. 6A) and relative proportions of PARAFAC components (Fig. 6B) between shaken and unshaken samples indicated no significant difference; results from unshaken samples are reported for the remainder of this manuscript.

3.3. DOM characterization of groundwater and surface water

The mean composition of groundwater fDOM varies widely across the study area, with samples from T-Sand and T-Clay showing typically different characteristics (Table 1). Groundwater from T-Sand is broadly characterized by (i) lower Abs_{254} and TF; (ii) lower fluorescence intensities (by peak picking) of TPH-like, FA-like and HA-like components; (iii) lower FI, XOM, TPH:FA and β:α; (iv) lower PARAFAC component loadings; (v) higher SUVA; (vi) higher HIX and HIX_{corr}; and (vii) higher proportions of C1 as compared to groundwater from T-Clay. T-Sand is also generally highly reducing, with, compared to T-Clay, relatively high Fe, low SO_4^{2-} and DOC, but similar As. These comparisons between T-Sand and T-Clay relate to the mean values and ranges observed, noting that the Mann-Whitney non-parametric test indicates that the full distributions of T-Sand and T-Clay datasets are statistically different at >95% confidence level only for DOC, TPH:FA and β:α (Table 1). Many of these parameters and the relationships between them will be discussed specifically. In general, the Holocene groundwater in this study has lower β:α, lower SUVA and much higher HIX than Holocene groundwater in the Bengal Basin (Kulkarni et al., 2017); this, combined with the broad variation observed within this study, suggests that some of the trends observed in Bengal aquifers may not necessarily be applicable to other shallow, reducing aquifers such as in Cambodia. Selected sample-specific data is shown for all pre-monsoon groundwater and surface water samples (Table 2).

There were also significant differences in fDOM properties observed between the groundwater and surface waters sampled, even though the range of values in total fluorescence was similar. These differences included that the surface water, as compared to groundwater, typically had: (i) lower TPH-like, FA-like, and HA-like components; (ii) higher FI; (iii) higher TPH-like and FA-like; and (iv) lower XOM and β:α. The composition between pond (SW-LR14) and river (SW-Bassac; SW-Mekong) surface waters also varied significantly. Compared to the river samples, the pond sample had: (i) much higher TPH-like, FA-like and HA-like components; (ii) lower FI; (iii) lower TPH:FA; and (iv) higher HI and XOM; and (v) higher β:α. The surface water samples may reflect differing contributions from base flow, soil runoff, water-rock interactions and anthropogenic activities, depending on the sample, locality and temporal variations, which may affect the fDOM and inorganic composition to varying degrees (Tye and Lapworth, 2016; Richards et al., 2017a).

Table 2
Absorbance-corrected fluorescence peak and selected fluorescence and absorbance indices and modelled PARAFAC components with parameters as defined in Table 1 for pre-monsoon groundwater (GW) from T-Sand and T-Clay and surface water (SW) samples; summary statistics are shown on Table 1; n/a indicates data not available.

Sample ID	Type	TPH-like$_{mean}$ (RU)	FA-like$_{mean}$ (RU)	HA-like$_{mean}$ (RU)	TPH:FA	HIX$_{corr}$	FI	XOM	β:α	C1 (RU)	C2 (RU)	C3 (RU)	TF (RU)
LR01-15	GW, T-Sand	0.31	0.96	0.77	0.32	0.94	1.55	0.08	0.58	1.66	1.20	0.21	3.1
LR01-21		0.89	2.81	2.50	0.32	0.94	1.31	0.21	0.57	5.64	3.73	0.70	10.1
LR01-30		0.79	2.01	1.70	0.39	0.93	1.23	0.16	0.57	3.88	2.67	0.65	7.2
LR01-45		0.74	2.17	1.92	0.34	0.95	1.36	0.18	0.53	4.48	2.96	0.60	8.0
LR01-6		0.54	0.59	0.44	0.92	0.85	1.10	0.05	0.64	1.10	0.77	0.43	2.3
LR01-9		1.76	5.21	4.28	0.34	0.94	1.33	0.39	0.56	9.99	7.08	1.42	18.5
LR02-15		0.25	0.85	0.68	0.29	0.93	1.34	0.08	0.54	1.49	1.00	0.20	2.7
LR02-30		1.12	3.35	2.74	0.34	0.94	1.35	0.26	0.62	6.34	4.59	0.86	11.8
LR03-15		0.65	2.41	1.89	0.27	0.95	1.37	0.21	0.53	4.18	2.98	0.43	7.6
LR04-15		1.24	3.97	3.25	0.31	0.95	1.23	0.29	0.54	7.63	5.52	0.97	14.1
LR04-30		1.16	3.12	2.55	0.37	0.94	1.15	0.25	0.58	5.97	4.49	0.90	11.4
LR05-15		1.55	4.70	4.03	0.33	0.94	1.29	0.35	0.60	9.30	6.66	1.24	17.2
LR05-21		1.20	4.16	3.61	0.29	0.94	1.27	0.34	0.54	8.07	5.39	0.97	14.4
LR05-30		1.37	4.29	3.37	0.32	0.94	1.26	0.31	0.57	7.82	5.75	1.08	14.7
LR05-6		0.23	0.53	0.35	0.43	0.93	1.84	0.05	0.77	0.82	0.74	0.16	1.7
LR05-9		2.84	5.10	4.42	0.56	0.91	1.24	0.44	0.57	10.67	7.02	2.34	20.0
LR07-15		0.58	1.77	1.36	0.33	0.93	1.29	0.15	0.63	3.00	2.38	0.46	5.8
LR07-30		1.86	6.08	5.07	0.31	0.94	1.27	0.40	0.61	11.60	8.71	1.58	21.9
LR08-30		1.33	4.05	3.18	0.33	0.94	1.36	0.28	0.61	7.23	5.55	1.08	13.9
LR09-21		3.49	11.19	8.88	0.31	0.94	1.40	0.59	0.56	20.04	15.13	2.59	37.8
LR09-30		2.02	6.19	5.12	0.33	0.94	1.30	0.47	0.63	n/a	n/a	n/a	n/a
LR09-45		0.53	1.38	1.10	0.39	0.93	1.12	0.14	0.65	2.52	2.00	0.41	4.9
LR09-6		0.22	0.62	0.45	0.35	0.93	0.93	0.06	0.64	1.15	0.83	0.17	2.2
LR10-15	GW, T-Clay	0.52	1.64	1.40	0.31	0.94	1.31	0.12	0.57	3.35	2.40	0.45	6.2
LR10-21		4.17	11.16	8.62	0.37	0.93	1.27	0.81	0.63	20.22	17.36	3.40	41.0
LR10-30		1.53	2.96	1.91	0.52	0.88	1.67	0.21	0.68	4.36	3.81	1.12	9.3
LR10-9		0.33	0.97	0.71	0.34	0.95	1.06	0.07	0.52	1.85	1.37	0.27	3.5
LR12-30		1.91	6.46	5.21	0.30	0.95	1.36	0.53	0.58	12.51	9.57	1.54	23.6
LR13-30		6.59	16.42	12.97	0.40	0.92	1.31	1.05	0.68	29.25	23.90	5.53	58.7
LR14-15		3.62	7.92	5.78	0.46	0.89	1.35	0.74	0.74	12.29	11.75	2.98	27.0
LR14-21		8.99	19.92	15.44	0.45	0.90	1.44	1.51	0.74	n/a	n/a	n/a	n/a
LR14-30		7.13	19.92	15.52	0.36	0.92	1.33	1.33	0.69	32.83	28.37	6.52	67.7
LR14-6		0.57	1.22	0.80	0.47	0.91	1.46	0.11	0.78	1.79	1.82	0.40	4.0
LR14-9		0.71	1.41	0.97	0.50	0.90	1.12	0.12	0.71	2.36	2.04	0.54	4.9
SW-LR14	SW	2.38	7.72	5.82	0.31	0.95	1.21	0.41	0.57	15.63	11.71	1.85	29.2
SW-Bassac		0.53	0.60	0.42	0.88	0.86	1.52	0.09	0.52	1.16	0.82	0.43	2.4
SW-Mekong		0.39	0.98	0.62	0.40	0.91	1.71	0.07	0.46	1.54	1.12	0.23	2.9

Overall depth against modelled total fluorescence (as the sum of PARAFAC components) shows further differences between T-Sand and T-Clay groundwater (Fig. 7A). On T-Clay, there is a strong positive correlation between depth and total fluorescence ($t(8) = 2.60$; $p < 0.05$), with the highest fluorescence values found on this transect. In contrast, the correlation on T-Sand is not statistically significantly, and interestingly the highest total fluorescence is instead observed at mid-depths, with low values obtained at both shallow and the deepest 45 m groundwater samples. It is difficult to ascertain the extent of this trend at depth given the limited number of samples obtained >30 m in depth, however this would be of interest to explore in future studies. Bulk DOC and total fluorescence (Fig. 7B) are strongly correlated for the entire dataset ($t(35) = 10.5$; $p < 0.05$), as would be reasonably expected given the significant proportion of OM that fluoresces (Bech et al., 1993; Hudson et al., 2007).

Depth profiles of various absorbance corrected fluorescence peak and selected indices further characterize the fDOM in groundwater (and surface water as indicated at 0 m depth) and show a number of other trends (Fig. 8). Similarly to the peak in TF at mid-depths, the maxima in TPH-like and HA-like fDOM are observed around 20 m in depth, with the maxima of FA-like fDOM observed slightly shallower, around 15 m in depth. TPH-like fDOM is typically much higher in T-Clay than in T-Sand. HA-like fDOM is also generally higher in T-Clay than in T-Sand, which may indicate more extensive microbial degradation of fDOM in T-Clay; a similar observation was made when comparing Holocene versus Pleistocene aquifers in the Bengal Basin (Kulkarni et al., 2017). Interestingly, FI increases with depth on T-Clay but not on T-Sand (Fig. 8D); typically lower values of FI (~1.3–1.4) indicate terrestrial fDOM sources whereas higher values of FI (~1.7–1.9) may be associated with inputs from microbial fDOM sources (McKnight et al., 2001; Cory and McKnight, 2005).

The β:α index has no apparent relationship with depth, however β:α is typically higher (e.g. containing more labile fDOM) in T-Clay than T-Sand (Fig. 8E). The higher β:α observed in T-Clay as compared to T-Sand is indicative of a greater input of autochthonous, indigenous carbon production, which is consistent with the generally clay-dominated lithology, and associated lower electrical resistivities and permeabilities encountered on this transect (Richards et al., 2017a; Uhlemann et al., 2017). In contrast, the lower β:α observed in T-Sand is indicative of greater possible input from external, surface derived sources to the fDOM pool, potentially via transport through zones of rapid recharge, which is consistent with indicators of rapid surface water incursion in some locations based on inorganic geochemistry (Richards et al., 2017a), relatively young apparent groundwater ages (Richards et al., 2017b) and the presence of near-surface sand windows (Uhlemann et al., 2017) along this transect. The β:α ratio is negatively correlated with HIX$_{corr}$ ($t(35) = -2.05$; $p < 0.05$) for the overall dataset; suggesting that the more labile fDOM has a lower degree of humicity, and thus the labile fDOM may be derived microbially rather than from recently lysed plant cells (Tye and Lapworth, 2016). Surface derived sources could plausibly contribute to the fDOM pool via vertical migration due to diffusive recharge and/or from surface water sources such as rivers or ponds (Lawson et al., 2013), especially depending on

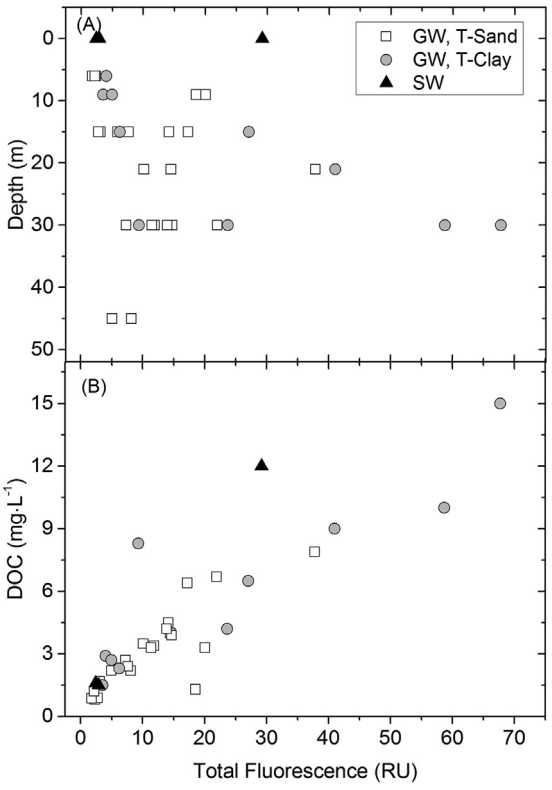

Fig. 7. (A) Depth and (B) bulk DOC versus total fluorescence calculated as the sum of PARAFAC components for groundwater from T-Sand (open square) and T-Clay (grey filled circle) and surface water (black filled triangle).

locality. Another possible external input to the fDOM pool could potentially be the influx of mature, petroleum-derived DOM from deeper down within the aquifer systems (van Dongen et al., 2008). Although there were no PAH components identified within the validated PARAFAC model, this does not necessarily mean that they are not present, but rather that the signal is too small to be modelled or significant. Interestingly the highest XOM indices were observed at site LR14 very near a pond (with also relatively elevated XOM; see Table 2) which suggests that surface-groundwater interactions may affect PAH components in the fDOM pool in some locations such as near ponds.

Interestingly, β:α is largely independent (at the 95% confidence interval) of both bulk DOC (Fig. 9A) and groundwater arsenic (Fig. 9C) for both T-Sand and T-Clay, despite the mobilization of arsenic having been linked with bioavailable DOM in a number of studies (Bhattacharya et al., 1997; Islam et al., 2004; Charlet and Polya, 2006; Postma et al., 2007; Rowland et al., 2009). The independence of β:α and bulk DOC is not surprising and it is generally recognized that even high levels of DOC do not necessarily mean that high levels of bioavailable DOC are present; indeed previous microcosm experiments have indeed shown that the amount of bulk OM present is not necessarily related to the amount of arsenic released (Rowland et al., 2009). However, if the presence of bioavailable DOM was a major control on arsenic release and arsenic was being mobilized exclusively in nearby locations to where it was observed in the water column, it would have been expected that a correlation between β:α and arsenic might be observed, while noting that complex processes including (partial) sorption/desorption and vertical and/or horizontal groundwater flow may also be simultaneously occurring and could be confounders affecting apparent associations between β:α and arsenic. A significant negative correlation between β:α and iron is observed exclusively on T-Clay (Fig. 9B). In addition to β:α, correlations between other fDOM indices and absorbance corrected mean fluorescence peaks and DOC, iron and arsenic for T-Sand, T-Clay and the overall dataset are summarized (Table 3). Within the overall dataset, positive correlations between HIX_{corr} and both iron and arsenic are observed (although this relationship does not hold for only the T-Sand subset is considered). For T-Sand, arsenic is correlated with each of TPH-like, HA-like and FA-like fDOM (although this is not observed for T-Clay). XOM is positively correlated with DOC, iron and arsenic on T-Sand, which is interesting considering that some of the sand-dominated sediments have been shown to contain thermally mature, petroleum-derived hydrocarbons (Magnone et al., 2017). Disentangling the differences between transects and understanding the apparent associated controls on arsenic mobilization remains the subject of ongoing investigations.

The differences in characteristic organic signatures between the transects can be further seen when comparing the FA-like intensities against TPH:FA (Fig. 10A). Groundwater from T-Clay typically has higher FA-like intensities, and T-Sand typically has a lower range of FA-like intensities combined with a much wider range of TPH:FA. The relatively low values of TPH:FA (e.g. $< \sim 0.4$) for most of the T-Sand samples suggest that these samples are not significantly impacted from fDOM derived from wastewater (Baker and Lamont-Black, 2001; Lapworth et al., 2008). Interestingly, however, the two samples on T-Sand with substantially higher TPH:FA (e.g. TPH:FA = 0.92 and 0.56) are from the shallowest 6 m depth; the sample containing the highest TPH:FA is located near a pig farm

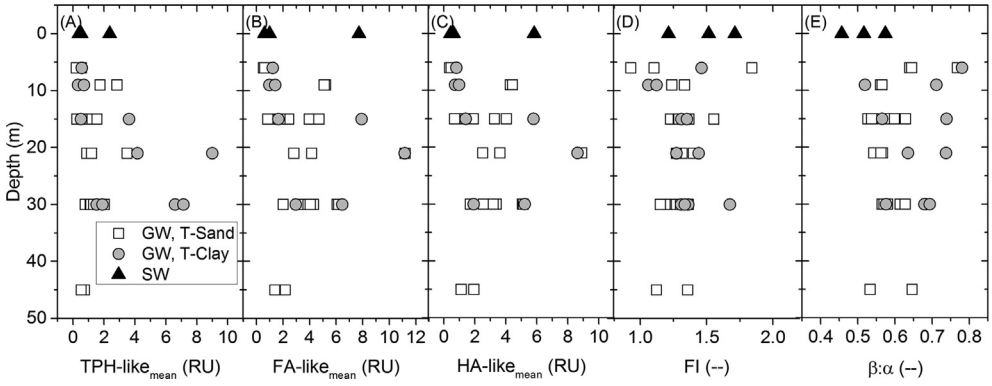

Fig. 8. Depth profiles for mean fluorescence peaks for (A) tryptophan-like (TPH-like); (B) fulvic acid-like (FA-like); (C) humic-acid like (HA-like) components; and for (D) fluorescence indices (FI) as defined by McKnight et al. (2001) and (E) β:α indices for groundwater from T-Sand (open square) and T-Clay (grey filled circle) and surface water (black filled triangle, shown at 0 m of depth).

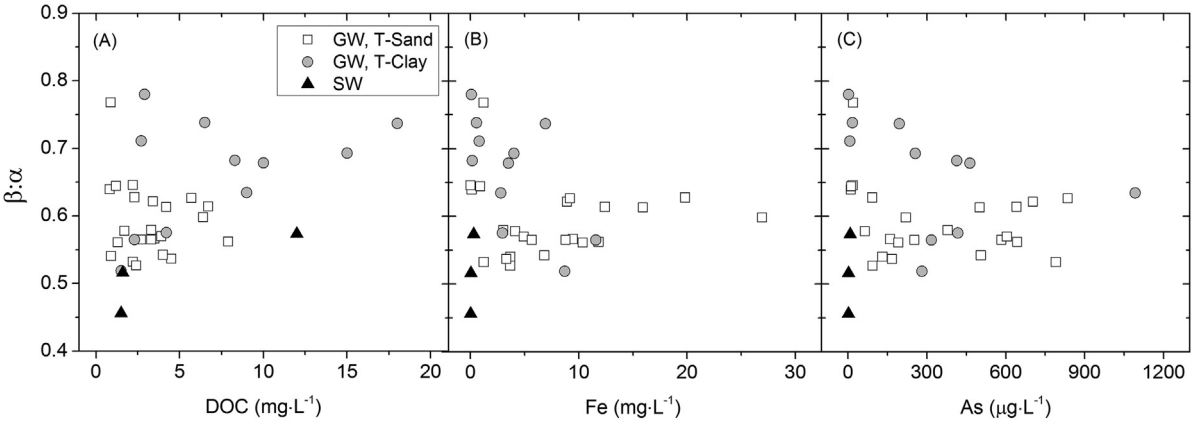

Fig. 9. Freshness index β:α versus (A) DOC, (B) iron, and (C) arsenic for groundwater from T-Sand (open square) and T-Clay (grey filled circle) and surface water (black filled triangle).

Table 3
Correlation *t*-values for DOC, iron and arsenic with selected fDOM indices and absorbance-corrected mean fluorescence peaks for groundwater from T-Sand ($n = 33$, degrees of freedom (df) = 21), T-Clay ($n = 11$, df = 9), and the overall dataset including surface water ($n = 37$, df = 35). Correlations are reported only where significant at the 95% confidence level ($p < 0.05$); '– 'indicates not significant at the 95% confidence level.

	DOC			Fe			As		
	T-Sand	T-Clay	Overall	T-Sand	T-Clay	Overall	T-Sand	T-Clay	Overall
β:α	–	–	2.37	–	−2.59	–	–	–	–
HIX_{corr}	–	–	–	–	2.31	2.24	–	–	2.12
FI	–	–	–	–	–	–	–	–	–
XOM	6.62	7.45	11.6	2.26	–	–	3.41	–	–
TPH-like	5.40	8.92	12.2	–	–	–	2.72	–	–
HA-like	7.76	6.92	12.3	2.29	–	–	3.33	–	–
FA-like	7.60	7.36	13.1	2.24	–	–	3.27	–	–

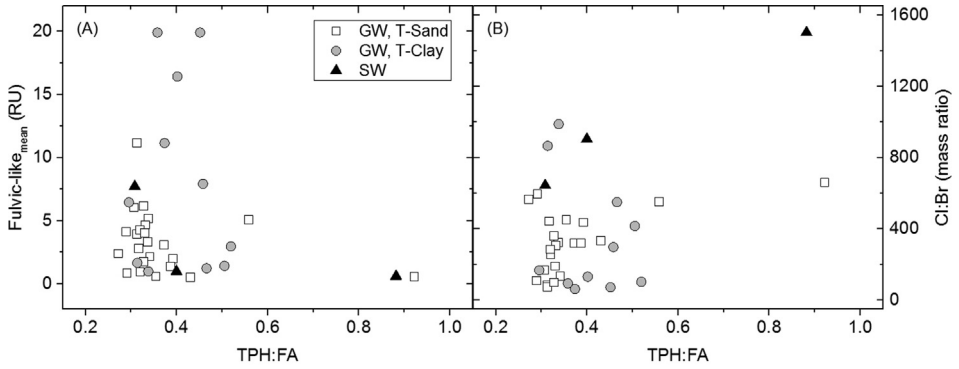

Fig. 10. (A) Mean fulvic-like intensity (RU) against the tryptophan:fulvic acid ratio (TPH:FA), as calculated from absorbance-corrected mean fluorescence peaks, for groundwater from T-Sand (open square) and T-Clay (grey filled circle) and surface water (black filled triangle); (B) Cl:Br mass ratio (Richards et al., 2018) against TPH:FA.

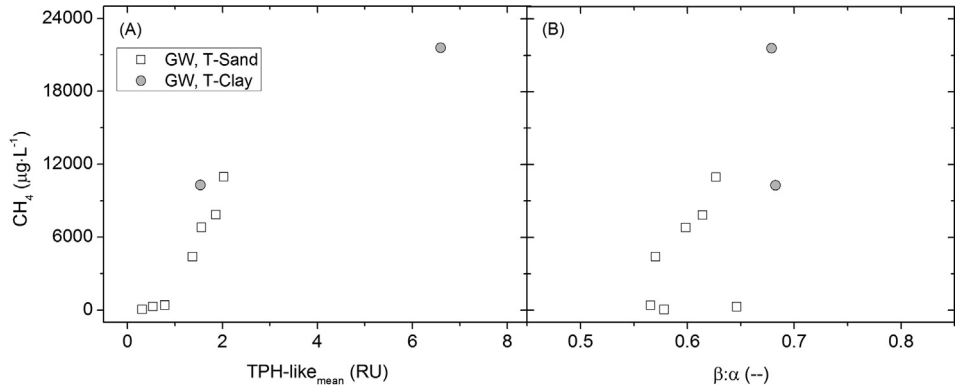

Fig. 11. Methane (CH_4) versus (A) mean tryptophan-like (TPH-like) intensity (RU) and (B) freshness indices β:α for selected groundwater samples from T-Sand (open square) and T-Clay (grey filled circle).

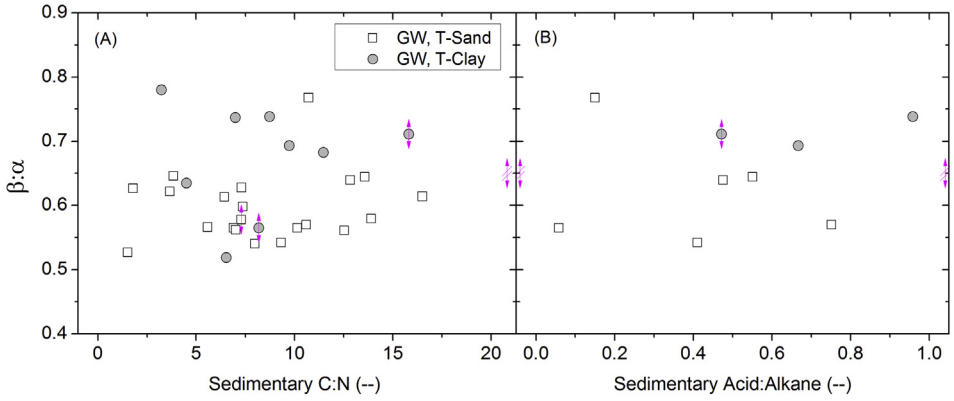

Fig. 12. Freshness index β:α for groundwater from T-Sand (open square) and T-Clay (grey filled circle) versus corresponding sedimentary bulk C:N and the ratio of high molecular weight (HWM) *n*-alkanoic acids or alcohols to HMW *n*-alkanes, as defined by HWM *n*-alkanoic acid (ng g^{-1})/Σ(HMW *n*-alkane (ng g^{-1}) + HMW *n*-alkanoic acid (ng g^{-1})) (Magnone et al., 2017).

and was also characterized by elevated Cl:Br ratios (Fig. 10B) and chloride (Richards et al., 2017a, 2018). The samples on T-Clay containing moderate TPH:FA in the range of ~0.4–0.5 are mostly from site LR14 located near a pond, and are also characterized by relatively high Cl:Br and chloride; together these observations are consistent with waste inputs plausibly resulting from pond-groundwater interactions (Lawson et al., 2013; Richards et al., 2017a, 2018; Kulkarni et al., 2018a). The surface water sample with substantially higher TPH:FA and Cl:Br as compared to other samples is from the Bassac River; such signatures are indicative of significant waste inputs.

3.4. Methane and DOM source characterization

Methane concentrations measured in a sub-set of samples ($n = 9$) varied greatly and ranged from ~60 to 22,000 μg L^{-1} (Fig. 11). The very high methane observed in some samples is generally consistent with the reducing conditions (Eh < 0 mV), low sulfate (<1 mg L^{-1}) and high alkalinity, although there is no universal methane proxy and baseline values can vary greatly (Gooddy and Darling, 2005; Darling and Gooddy, 2006; Bell et al., 2017). Three samples contained methane exceeding the suggested risk action levels of 10,000 μg L^{-1} (Eltschlager et al., 2001; Bell et al., 2017). To the authors' knowledge no baseline study of methane concentrations in groundwater in Cambodia exist; a more extensive survey of groundwater methane in this field area would be interesting especially given the wide variability noted in this subset.

Most methane in groundwater is derived from either bacterial/biogenic or thermal/thermogenic activity (Schoell, 1988), of which potential sources can be deduced via association with other geochemical parameters. A strong correlation between methane and TPH (Fig. 11A); (t (7) = 6.70; $p < 0.05$) suggests that the methane is likely of biogenic origin. This is further supported by the molar methane:ethane ("C_1:C_2") ratios in this study which were all > 3000 (data not shown), far exceeding the typically cut-off of C_1:C_2 > 1000 associated with biogenic methane production (Schoell, 1983). The formation of biogenic methane may be reasonably expected to be associated with the bioavailability of the fDOM present and likely to be undergoing methanogenesis (Gooddy and Darling, 2005). Indeed an overall correlation between methane and β:α is observed (t (7) = 2.51; $p < 0.05$) (Fig. 11B). The high concentrations of methane especially observed in T-Clay are consistent with the higher HA-like fDOM observed in this transect, and is suggestive of more extensive microbial degradation of fDOM in T-Clay than in T-Sand groundwater. The overall correlation between methane and HA-like fDOM is significant (t (7) = 5.73; $p < 0.05$). An important extension of this argument is that the likely methanogenesis occurring, particularly in T-Clay, may lead to a substantial consumption of organic carbon (Postma et al., 2016), further limiting its availability for other microbially-mediated processes including reductive dissolution of arsenic bearing iron minerals. This plausibly suggests that even in reducing, arsenic-prone environments where bioavailable OM sources are present, confounding processes like methanogenesis may provide additional controls on the rate or extent which further arsenic mobilization occurs. More detailed discussion on the potential impact of methanogenesis and geochemical evidence for the dual role of in-aquifer and near surface processes in driving arsenic mobilization in this study area is published elsewhere (Richards et al., 2019a).

3.5. Comparison between aqueous and sedimentary OM proxies

Interestingly, there is no apparent correlation between groundwater β:α and corresponding sedimentary proxies/biomarkers, namely the bulk sedimentary C:N ratio (ranging 1.5–16.5) and the ratio of high molecular weight (HWM) *n*-alkanoic acids or alcohols to HMW *n*-alkanes (ranging 0.06–0.96) (Magnone et al., 2017) (Fig. 12). Again, the confounders mentioned above including the potential role of (partial) equilibrium (Richards et al., 2019b) and/or hydrological processes may complexly influence the sedimentary and corresponding aqueous OM proxies even in the same location. The bulk sedimentary C:N ratio can be used to help distinguish the origin of sedimentary organic matter (SOM), with higher sedimentary C:N ratios typically associated with plant-derived SOM (Lamb et al., 2006; Magnone et al., 2017). However, there is also no correlation between C:N and aqueous HIX_{corr} (data not shown). The ratio of HMW acid:alkane, as defined here by HWM *n*-alkanoic acid/Σ(HMW *n*-alkane + HMW *n*-alkanoic acid), is a robust SOM degradation proxy indicating the relative degree of oxidation for materials of similar origin. The carbon preference index is used first to distinguish thermally mature/petroleum-derived versus immature/plant-derived SOM sources, prior to estimating the degree of oxidation of plant-derived samples with the HMW acid:alkane ratio (Poynter and Eglinton, 1990; Marzi et al., 1993; van Dongen et al., 2006; Vonk et al., 2008; Magnone et al., 2017). The HMW acid:alkane proxy is based on the well-known SOM degradation pathway from alkanes (the most reduced) eventually to alkanoic acids and inorganic carbon (the most oxidized) (Magnone et al., 2017 and references within). In the same study area, for thermally immature samples, the HMW

acid:alkane in the early (>6000 year), mixed lithology, Holocene facies is higher (thus indicating higher levels of oxidation) than in the young (<2000 year), clay-dominant Holocene facies, which could be associated with the time available for degradation or differences in bioavailability (Magnone et al., 2017). Thermally mature, petroleum-derived hydrocarbons were observed previously in some sandy sediments from this study area (Magnone et al., 2017), which may contribute to the XOM indices observed in groundwater samples (even though the signals of a PAH-component were too low to be validated in PARAFAC modelling). The observation that there is no apparent overall relationship between the aqueous β:α and the corresponding (e.g. at the same depth and location) selected SOM proxies (Fig. 12) is interesting, and is consistent with the suggestion that there may be external contributions (e.g. surface-derived and/or petroleum-derived from deeper within the aquifers) to the aqueous DOM pool rather than exclusively contributions from the directly surrounding sedimentary environment. This is consistent with the hypothesis that external, modern surface-derived DOM, largely from ponds, rivers and rice paddies may be an important control on groundwater geochemistry, including arsenic mobilization, in some settings (Harvey et al., 2002; Kocar et al., 2008; Papacostas et al., 2008; Polizzotto et al., 2008; Neumann et al., 2010; Lawson et al., 2013, 2016).

4. Conclusions

The aqueous organic matter pool in a heavily arsenic affected aquifer in northern Kandal Province, Cambodia has been characterized for the first time using EEM fluorescence spectroscopy and PARAFAC modelling. Groundwaters were generally dominated by terrestrial HA-like and FA-like components, with relatively small contributions from microbial-derived TPH-like components. Selected absorbance-corrected fluorescence indices were used to characterize differences in the DOM pools with depth and to compare groundwaters from distinct transects. Groundwater from sand-dominated sequences typically contained lower TPH-like, FA-like and HA-like components, and had lower FI and β:α, and higher humification as compared to clay-dominated sequences. Fluorescence DOM in surface waters and groundwater varied greatly across the field area and depends on the origin of the water, other potential inputs and extent of water-rock interactions, amongst other factors. Methane concentrations were strongly correlated with fDOM bioavailability as well as TPH-like components, suggesting that methane is likely of biogenic origin. High concentrations of methane, especially in clay-dominated sequences, are consistent with higher HA-like fDOM present and are suggestive of more extensive microbial degradation of DOM in T-Clay than in groundwaters from sand-dominated sequences. Methanogenesis likely leads to a substantial consumption of organic carbon, which may provide an additional control of the rate or extent to which arsenic is mobilized via microbially-mediated reductive dissolution processes in these areas. DOM bioavailability was not correlated with bulk DOC, arsenic, or sedimentary proxies of SOM degradation in corresponding locations. Whilst not definitive, this is consistent with the hypothesis that external, surface-derived contributions to the aqueous DOM pool may be an important control on groundwater geochemistry.

Acknowledgements

This research was funded by a NERC Standard Research Grant (NE/J023833/1) to DAP, BvD and Christopher Ballentine (now at University of Oxford), with additional support from the Leverhulme Trust (ECF2015-657) to LAR, a NERC PhD studentship (NE/L501591/1) to DM and a NERC Collaborative Awards in Science and Engineering PhD studentship (NE/501736/1) to LC. We are very grateful to Chansopheaktra Sovann (Royal University of Phnom Penh, Cambodia), Chivuth Kong (now at Royal University of Agriculture, Cambodia) and the field assistants (Pheary Meas and Yut Yann, both formerly Royal University of Agriculture) contributing to the field campaigns relevant to this manuscript. Hok Meas and drilling team, local tenants and landowners, and Resources Development International-Cambodia are thanked for their support of field activities. Paul Lythgoe and Alastair Bewsher (both The University of Manchester) are thanked for ICP and IC analytical support. DJL, DCG and PJW publish with the permission of the Executive Director, British Geological Survey (NERC).

References

Al Lawati, W.M., Jean, J.-S., Kulp, T.R., Lee, M.-K., Polya, D.A., Liu, C.-C., van Dongen, B.E., 2013. Characterisation of organic matter associated with groundwater arsenic in reducing aquifers of southwestern Taiwan. Journal of Hazardous Materials 262, 970–979.

Al Lawati, W.M., Rizoulis, A., Eiche, E., Boothman, C., Polya, D.A., Lloyd, J.R., Berg, M., Vasquez-Aguilar, P., van Dongen, B.E., 2012. Characterisation of organic matter and microbial communities in contrasting arsenic-rich Holocene and arsenic-poor Pleistocene aquifers, Red River Delta, Vietnam. Applied Geochemistry 27, 315–325.

Baker, A., 2001. Fluorescence excitation-emission matrix characterization of some sewage-impacted rivers. Environmental Science and Technology 35, 948–953.

Baker, A., 2002. Fluorescence properties of some farm wastes: implications for water quality monitoring. Water Research 36, 189–195.

Baker, A., Curry, M., 2004. Fluorescence of leachates from three contrasting landfills. Water Research 38, 2605–2613.

Baker, A., Lamont-Black, J., 2001. Fluorescence of dissolved organic matter as a natural tracer of ground water. Ground Water 39, 745–750.

Bauer, M., Blodau, C., 2006. Mobilization of arsenic by dissolved organic matter from iron oxides, soils and sediments. The Science of the Total Environment 354, 179–190.

Bech, A.J., Jones, K.C., Hayes, M.B.H., Mingelgrin, U., 1993. Organic Substances in Soil and Water: Natural Constituents and Their Influences on Contaminant Behaviour. The Royal Society of Chemistry.

Bell, R.A., Darling, W.G., Ward, R.S., Basava-Reddi, L., Halwa, L., Manamsa, K., Ó Dochartaigh, B.E., 2017. A baseline survey of dissolved methane in aquifers of Great Britain. The Science of the Total Environment 601 – 602, 1803–1813.

Benedetti, M.F., van Riemsdijk, W.H., Kooral, L.K., Kinniburgh, D.G., Gooddy, D.C., Milne, C.J., 1996. Metal ion binding by natural organic matter: from the model to the field. Geochimica et Cosmochimica Acta 60, 2503–2513.

Benner, S.G., Polizzotto, M.L., Kocar, B.D., Ganguly, S., Phan, K., Ouch, K., Sampson, M., Fendorf, S., 2008. Groundwater flow in an arsenic-contaminated aquifer, Mekong Delta, Cambodia. Applied Geochemistry 23, 3072–3087.

Bhattacharya, P., Chatterjee, D., Jacks, G., 1997. Occurrence of arsenic contaminated groundwater in alluvial aquifers from Delta plains, Eastern India: options for safe drinking water supply. Water Resources Development 13, 79–92.

Birdwell, J.E., Valsaraj, K.T., 2010. Characterization of dissolved organic matter in fogwater by excitation-emission matrix fluorescence spectroscopy. Atmospheric Environment 44, 3246–3253.

Bro, R., 1997. PARAFAC. Tutorial and applications. Chemometrics and Intelligent Laborary Systems 38, 149–171.

Cannavo, P., Dudal, Y., Boudenne, J.-L., Lafolie, F., 2004. Potential for fluorescence spectroscopy to assess the quality of soil water-extracted organic matter. Soil Science 169, 688–696.

Charlet, L., Polya, D.A., 2006. Arsenic in shallow, reducing groundwaters in southern Asia: an environmental health disaster. Elements 2, 91–96.

Chen, J., Gu, B., Leboeuf, E.J., Pan, H., Dai, S., 2002. Spectroscopic characterization of the structural and functional properties of natural organic matter fractions. Chemosphere 48, 59–68.

Chen, J., Leboeuf, E.J., Dai, S., Gu, B., 2003a. Fluorescence spectroscopic studies of natural organic matter fractions. Chemosphere 50, 639–647.

Chen, W., Westerhoff, P., Leenheer, J.A., Booksh, K., 2003b. Fluorescence excitation-emission matrix regional integration to quantify spectra for dissolved organic matter. Environmental Science and Technology 37, 5701–5710.

Coble, P.G., 1996. Characterization of marine and terrestrial DOM in seawater using excitation-emission matrix spectroscopy. Marine Chemistry 51, 325–346.

Cory, R.M., McKnight, D.M., 2005. Fluorescence spectroscopy reveals ubiquitous presence of oxidized and reduced quinones in dissolved organic matter. Environmental Science and Technology 39, 8142–8149.

Darling, W.G., Gooddy, D.C., 2006. The hydrogeochemistry of methane: evidence from English groundwaters. Chemical Geology 229, 293–312.

Datta, S., Neal, A.W., Mohajerin, T.J., Ocheltree, T., Rosenheim, B.E., White, C.D., Johannesson, K.H., 2011. Perennial ponds are not an important source of water or dissolved organic matter to groundwaters with high arsenic concentrations

in West Bengal, India. Geophysical Research Letters 38, L20404. https://doi.org/10.1029/2011GL049301.
Davis, J., Benner, R., 2007. Quantitative estimates of labile and semi-labile dissolved organic carbon in the western Arctic Ocean: a molecular approach. Limnology & Oceanography 52, 2434–2444.
Del Castillo, C.E., Coble, P.G., Morell, J.M., López, J.M., Corredor, J.E., 1999. Analysis of the optical properties of the Orinoco River plume by absorption and fluorescence spectroscopy. Marine Chemistry 66, 35–51.
Eltschlager, K.K., Hawkins, J.W., Ehler, W.C., Baldassare, F., 2001. Technical Measures for the Investigation and Mitigation of Fugitive Methane Hazards in Areas of Coal Mining.
Gooddy, D.C., Darling, W.G., 2005. The potential for methane emissions from groundwaters of the UK. The Science of the Total Environment 339, 117–126.
Gustaffson, J.P., 2006. Arsenate adsorption to soils: modelling the competition from humic substances. Geoderma 136, 320–330.
Hall, G.J., Clow, K.E., Kenny, J.E., 2005. Estuarial fingerprinting through multidimensional fluorescence and multivariate analysis. Environmental Science and Technology 39, 7560–7567.
Harvey, C.F., Swartz, C.H., Badruzzaman, A.B.M., Keon-Blute, N., Yu, W., ASHRAF Ali, M., Jay, J., Beckie, R., Niedan, V., Brabander, D., Oates, P.M., Ashfaque, K.N., Islam, S., Hemond, H.F., Ahmed, M.F., 2002. Arsenic mobility and groundwater extraction in Bangladesh. Science 298, 1602–1606.
Helms, J.R., Stubbins, A., Ritchie, J.D., Minor, E.C., Kieber, D.J., Mopper, K., 2008. Absorption spectral slopes and slope ratios as indicators of molecular weight, source, and photobleaching of chromophoric dissolved organic matter. Limnology & Oceanography 53, 955–969.
Her, N., Amy, G., McKnight, D., Sohn, J., Yoon, Y., 2003. Characterization of DOM as a function of MW by fluorescence EEM and Hplc-SEC using Uva, Doc, and fluorescence detection. Water Research 37, 4295–4303.
Holbrook, R.D., Yen, J.H., Grizzard, T.J., 2006. Characterizing natural organic material from the Occoquan Watershed (Northern Virginia, US) using fluorescence spectroscopy and PARAFAC. The Science of the Total Environment 361, 249–266.
Huang, S., Wang, Y., Ma, T., Tong, L., Wang, Y., Liu, C., Zhao, L., 2015. Linking groundwater dissolved organic matter to sedimentary organic matter from a fluvio-lacustrine aquifer at Jianghan Plain, China by Eem-PARAFAC and hydrochemical analyses. The Science of the Total Environment 529, 131–139.
Hudson, N., Baker, A., Reynolds, D., 2007. Fluorescence analysis of dissolved organic matter in natural, waste and polluted waters - a review. River Research and Applications 23, 631–649.
Huo, S., Xi, B., Yu, H., He, L., Fan, S., Liu, H., 2008. Characteristics of dissolved organic matter (DOM) in leachate with different landfill ages. Journal of Environmental Sciences 20, 492–498.
Islam, F.S., Gault, A.G., Boothman, C., Polya, D.A., Charnock, J.M., Chatterjee, D., Lloyd, J.R., 2004. Role of metal-reducing bacteria in arsenic release from Bengal Delta sediments. Nature 430, 68–71.
Jiang, J., Bauer, I., Paul, A., Kappler, A., 2009. Arsenic redox changes by microbially and chemically formed semiquinone radicals and hydroquinones in a humic substance model quinone. Environmental Science and Technology 43, 3639–3645.
Jiang, J., Kappler, A., 2008. Kinetics of microbial and chemical reduction of humic substances: implications for electron shuttling. Environmental Science and Technology 42, 3563–3569.
Kappler, A., Benz, M., Schink, B., Brune, A., 2004. Electron shuttling via humic acids in microbial iron(III) reduction in a freshwater sediment. FEMS Microbiology Ecology 47, 85–92.
Katsuyama, M., Ohte, N., 2002. Determining the sources of stormflow from the fluorescence properties of dissolved organic carbon in a forested headwater catchment. Journal of Hydrology 268, 192–202.
Kelleher, B.P., Simpson, A.J., 2006. Humic substances in soils: are they really chemically distinct? Environmental Science and Technology 40, 4605–4611.
Klapper, L., McKnight, D.M., Fulton, J.R., Blunt-Harris, E.L., Nevin, K.P., Lovley, D.R., Hatcher, P.G., 2002. Fulvic acid oxidation state detection using fluorescence spectroscopy. Environmental Science and Technology 36, 3170–3175.
Kleber, M., Johnson, M.G., 2010. Advances in understanding the molecular structure of soil organic matter: implications for interactions in the environment. Advances in Agronomy 106, 77–142.
Ko, I., Kim, J.-Y., Kim, K.-W., 2004. Arsenic speciation and sorption kinetics in the As-hematite-humic acid system. Colloids and Surfaces A: Physicochemical and Engineering Aspects 234, 43–50.
Kocar, B.D., Polizzotto, M.L., Benner, S.G., Ying, S.C., Ung, M., Ouch, K., Samreth, S., Suy, B., Phan, K., Sampson, M., Fendorf, S., 2008. Integrated biogeochemical and hydrologic processes driving arsenic release from shallow sediments to groundwaters of the Mekong Delta. Applied Geochemistry 23, 3059–3071.
Kowalczuk, P., Cooper, W.J., Durako, M.J., Kahn, A.E., Gonsior, M., Young, H., 2010. Characterization of dissolved organic matter fluorescence in the South Atlantic Bight with use of PARAFAC model: relationships between fluorescence and its components, absorption coefficients and organic carbon concentrations. Marine Chemistry 118, 22–36.
Kulkarni, H., Mladenov, N., Datta, S., 2019. Effects of acidification on the optical properties of dissolved organic matter from high and low arsenic groundwater and surface water. The Science of the Total Environment 653, 1326–1332.
Kulkarni, H.V., Mladenov, N., Datta, S., Chatterjee, D., 2018a. Influence of monsoonal recharge on arsenic and dissolved organic matter in the Holocene and Pleistocene aquifers of the Bengal Basin. The Science of the Total Environment 637 – 638, 588–599.
Kulkarni, H.V., Mladenov, N., Johannesson, K.H., Datta, S., 2017. Contrasting dissolved organic matter quality in groundwater in Holocene and Pleistocene aquifers and implications for influencing arsenic mobility. Applied Geochemistry 77.
Kulkarni, H.V., Mladenov, N., McKnight, D.M., Zheng, Y., Kirk, M.F., Nemergut, D.R., 2018b. Dissolved fulvic acids from a high arsenic aquifer shuttle electrons to enhance microbial iron reduction. The Science of the Total Environment 615, 1390–1395.
Lakowicz, J.R., 1991. Topics in Fluorescence Spectroscopy. Springer.
Lamb, A.L., Wilson, G.P., Leng, M.J., 2006. A review of coastal palaeoclimate and relative sea-level reconstructions using $\Delta^{13}C$ and C/N ratios in organic material. Earth-Science Reviews 75, 29–57.
Lapworth, D.J., Gooddy, D.C., Allen, D., Old, G.H., 2009. Understanding groundwater, surface water, and hyporheic zone biogeochemical processes in a Chalk catchment using fluorescence properties of dissolved and colloidal organic matter. Journal of Geophysical Research 114, G00F02.
Lapworth, D.J., Gooddy, D.C., Butcher, A.S., Morris, B.L., 2008. Tracing groundwater flow and sources of organic carbon in sandstone aquifers using fluorescence properties of dissolved organic matter (DOM). Applied Geochemistry 23, 3384–3390.
Lapworth, D.J., Kinniburgh, D.G., 2009. An R script for visualising and analysing fluorescence excitation-emission matrices (EEMs). Computers & Geosciences 35, 2160–2163.
Lawrence, A.R., Gooddy, D.C., Kanatharana, P., Ramnarong, V., Meesilp, W., 2000. Groundwater evolution beneath Hat Yai, a rapidly developing city in Thailand. Hydrogeology Journal 8, 564–575.
Lawson, M., Polya, D.A., Boyce, A.J., Bryant, C., Ballentine, C.J., 2016. Tracing organic matter composition and distribution and its role on arsenic release in shallow Cambodian groundwaters. Geochimica et Cosmochimica Acta 178, 160–177.
Lawson, M., Polya, D.A., Boyce, A.J., Bryant, C., Mondal, D., Shantz, A., Ballentine, C.J., 2013. Pond-derived organic carbon driving changes in arsenic hazard found in Asian groundwaters. Environmental Science and Technology 47, 7085–7094.
Leenheer, J.A., Croué, J.-P., 2003. Characterizing Dissolved Aquatic Organic Matter. Environmental Science and Technology, p. 19A.
Lehmann, J., Kleber, M., 2015. The contentious nature of soil organic matter. Nature 528, 60–68.
Lehmann, J., Solomon, D., Kinyangi, J., Dathe, L., Wirick, S., Jacobsen, C., 2008. Spatial complexity of soil organic matter forms at nanometre scales. Nature Geoscience 1, 238–242.
Liu, G., Fernandez, A., Cai, Y., 2011. Complexation of arsenite with humic acid in the presence of ferric iron. Environmental Science and Technology 45, 3210–3216.
Lovley, D.R., Coates, J.D., Blunt-Harris, E.L., Phillips, E.J.P., Woodward, J.C., 1996. Humic substances as electron acceptors for microbial respiration. Nature 382, 445–448.
Lovley, D.R., Fraga, J.L., Blunt-Harris, E.L., Hayes, L.A., Phillips, E.J.P., Coates, J.D., 1998. Humic substances as a mediator for microbially catalyzed metal reduction. Acta Hydrochimica et Hydrobiologica 26, 152–157.
Lovley, D.R., Fraga, J.L., Coates, J.D., Blunt-Harris, E.L., 1999. Humics as an electron donor for anaerobic respiration. Environmental Microbiology 1, 89–98.
Magnone, D., Richards, L.A., Polya, D.A., Bryant, C., Jones, M., van Dongen, B.E., 2017. Biomarker-indicated extent of oxidation of plant-derived organic carbon (OC) in relation to geomorphology in an arsenic contaminated Holocene aquifer. Cambodia. Scientific Reports 7.
Mariot, M., Dudal, Y., Furian, S., Sakamoto, A., Vallès, V., Fort, M., Barbiero, L., 2007. Dissolved organic matter fluorescence as a water-flow tracer in the tropical wetland of Pantanal of Nhecolândia, Brazil. The Science of the Total Environment 388, 184–193.
Marzi, R., Torkelson, B.E., Olson, R.K., 1993. A revised carbon preference index. Organic Geochemistry 20, 1303–1306.
Matthews, B.J.H., Jones, A.C., Theodorou, N.K., Tudhope, A.W., 1996. Excitation-emission-matrix fluorescence spectroscopy applied to humic acid bands in coral reefs. Marine Chemistry 55, 317–332.
McArthur, J.M., Banerjee, D.M., Hudson-Edwards, K.A., Mishra, R., Purohit, R., Ravenscroft, P., Cronin, A., Howarth, R.J., Chatterjee, A., Talukder, T., Lowry, D., Houghton, S., Chadha, D.K., 2004. Natural organic matter in sedimentary basins and its relation to arsenic in anoxic ground water: the example of West Bengal and its worldwide implications. Applied Geochemistry 19, 1255–1293.
McArthur, J.M., Ravenscroft, P., Sracek, O., 2011. Aquifer arsenic source. Nature Geoscience 4, 655–656.
McKnight, D.M., Bencala, K.E., Zellweger, G.W., Aiken, G.R., Feder, G.L., Thorn, K.A., 1992. Sorption of dissolved organic carbon by hydrous aluminum and iron oxides occurring at the confluence of Deer Creek with the Snake River, Summit County, Colorado. Environmental Science and Technology 26, 1388–1396.
McKnight, D.M., Boyer, E.W., Westerhoff, P.K., Doran, P.T., Kulbe, T., Andersen, D.T., 2001. Spectrofluorometric characterization of dissolved organic matter for indication of precursor organic material and aromaticity. Limnology & Oceanography 46, 38–48.
Mikutta, C., Kretzschmar, R., 2011. Spectroscopic evidence for ternary complex formation between arsenate and ferric iron complexes of humic substances. Environmental Science and Technology 45, 9550–9557.
Miller, J.N., Miller, J.C., 2010. Chapter 5: Calibration Methods in Instrumental Analysis: Regression and Correlation. Statistics and Chemometrics for Analytical Chemistry. Pearson Education.

Mladenov, N., Zheng, Y., Miller, M.P., Nemergut, D.R., Legg, T., Simone, B., Hageman, C., Rahman, M.M., Ahmed, K.M., McKnight, D.M., 2010. Dissolved organic matter sources and consequences for iron and arsenic mobilization in Bangladesh aquifers. Environmental Science and Technology 44, 123–128.

Mladenov, N., Zheng, Y., Simone, B., Bilinski, T.M., McKnight, D.M., Nemergut, D., Radloff, K.A., Rahman, M.M., Ahmed, K.M., 2015. Dissolved organic matter quality in a shallow aquifer of Bangladesh: implications for arsenic mobility. Environmental Science and Technology 49, 10815–10824.

Mopper, K., Schultz, C.A., 1993. Fluorescence as a possible tool for studying the nature and water column distribution of DOC components. Marine Chemistry 41, 229–238.

Murphy, K.R., Hambly, A., Singh, S., Henderson, R.K., Baker, A., Stuetz, R., Khan, S.J., 2011. Organic matter fluorescence in municipal water recyclin schemes: toward a unified PARAFAC model. Environmental Science and Technology 45, 2909–2916.

Murphy, K.R., Stedmon, C.A., Graeber, D., Bro, R., 2013. Fluorescence spectroscopy and multi-way techniques. PARAFAC. Analytical Methods 5, 6541–6882.

Murphy, K.R., Stedmon, C.A., Waite, T.D., Ruiz, G.M., 2008. Distinguishing between terrestrial and autochthonous organic matter sources in marine environments using fluorescence spectroscopy. Marine Chemistry 108, 40–58.

Naden, P.S., Old, G.H., Eliot-Laize, C., Granger, S.J., Hawkins, J.M.B., Bol, R., Haygarth, P., 2010. Assessment of natural fluorescence as a tracer of diffuse agricultural pollution from slurry spreading on intensely-farmed grasslands. Water Research 44, 1701–1712.

Neumann, R.B., Ashfaque, K.N., Badruzzaman, A.B.M., Ali, M.A., Shoemaker, J.K., Harvey, C.F., 2010. Anthropogenic influences on groundwater arsenic concentrations in Bangladesh. Nature Geoscience 3, 46–52.

Neumann, R.B., Ashfaque, K.N., Badruzzaman, A.B.M., Ali, M.A., Shoemaker, J.K., Harvey, C.F., 2011. Aquifer arsenic source reply. Nature Geoscience 4 (10), 656.

Neumann, R.B., Polizzotto, M.L., Badruzzaman, A.B.M., Ali, M.A., Zhang, Z.Y., Harvey, C.F., 2009. Hydrology of a groundwater-irrigated rice field in Bangladesh: seasonal and daily mechanisms of infiltration. Water Resources Research 45, 14.

Nevin, K.P., Lovley, D.R., 2000. Lack of production of electron-shuttling compounds or solubilization of Fe(III) during reduction of insoluble Fe(III) oxide by *Geobacter metallireducens*. Applied and Environmental Microbiology 66, 2248–2251.

Nickson, R.T., McArthur, J.M., Burgess, W.G., Ahmed, K.M., Ravenscroft, P., Rahman, M., 1998. Arsenic poisoning of Bangladesh groundwater. Nature 395, 338.

Ohno, T., 2002. Fluorescence inner-filtering correction for determining the humification index of dissolved organic matter. Environmental Science and Technology 36, 742–746.

Ohno, T., Chorover, J., Omoike, A., Hunt, J., 2007. Molecular weight and humification index as predictors of adsorption for plant- and manure-derived dissolved organic matter to goethite. European Journal of Soil Science 58, 125–132.

Old, G.H., Naden, P.S., Granger, S.J., Bilotta, G.S., Brazier, R.E., Macleod, C.J.A., Krueger, T., Bol, R., Hawkins, J.M.B., Haygarth, P., Freer, J., 2012. A novel application of natural fluorescence to understand the sources and transport pathways of pollutants from livestock farming in small headwater catchments. The Science of the Total Environment 417 – 418, 169–182.

Papacostas, N.C., Bostick, B., Quicksall, A.N., Landis, J.D., Sampson, M., 2008. Geomorphic controls on groundwater arsenic distribution in the Mekong River Delta, Cambodia. Geology 36, 891–894.

Parker, C.A., Barnes, W.J., 1957. Some experiments with spectrofluorimeters and filter fluorimeters. Analyst 82, 606–618.

Parlanti, E., Wörz, K., Geoffroy, L., Lamotte, M., 2000. Dissolved organic matter fluorescence spectroscopy as a tool to estimate biological activity in a coastal zone submitted to anthropogenic inputs. Organic Geochemistry 31, 1765–1781.

Polizzotto, M.L., Kocar, B.D., Benner, S.G., Sampson, M., Fendorf, S., 2008. Near-surface wetland sediments as a source of arsenic release to ground water in Asia. Nature 454, 505–508.

Polya, D.A., Charlet, L., 2009. Rising arsenic risk? Nature Geoscience 2, 383–384.

Polya, D.A., Gault, A.G., Bourne, N.J., Lythgoe, P.R., Cooke, D.A., 2003. Coupled Hplc-Icp-MS Analysis Indicates Highly Hazardous Concentrations of Dissolved Arsenic Species in Cambodian Groundwaters, vol. 288. Royal Society of Chemistry Special Publication, pp. 127–140.

Polya, D.A., Gault, A.G., Diebe, N., Feldman, P., Rosenboom, J.W., Gilligan, E., Fredericks, D., Milton, A.H., Sampson, M., Rowland, H.A.L., Lythgoe, P.R., Jones, J.C., Middleton, C., Cooke, D.A., 2005. Arsenic hazard in shallow Cambodian groundwaters. Mineralogical Magazine 69, 807–823.

Polya, D.A., Richards, L.A., AL Bualy, A.N., Sovann, C., Magnone, D., Lythgoe, P.R., 2017. Chapter A14: groundwater sampling, arsenic analysis and risk communication: Cambodia Case Study. In: Bhattacharya, P., Polya, D.A., Jovanovic, D. (Eds.), Best Practice Guide for the Control of Arsenic in Drinking Water (ISBN13: 9781843393856). IWA Publishing.

Postma, D., Larsen, F., MINH Hue, N.T., Duc, M.T., Viet, P.H., Nhan, P.Q., Jessen, S., 2007. Arsenic in groundwater of the Red River floodplain, Vietnam: controlling geochemical processes and reactive transport modeling. Geochimica et Cosmochimica Acta 71, 5054–5071.

Postma, D., Trang, P.T.K., Sø, H.U., Hoan, H.V., Lan, V.M., Thai, N.T., Larsen, F., Viet, P.H., Jakobsen, R., 2016. A model for the evolution in water chemistry of an arsenic contaminated aquifer over the last 6000 years, Red River floodplain, Vietnam. Geochimica et Cosmochimica Acta 195, 277–292.

Poynter, J., Eglinton, G., 1990. Molecular composition of three sediments from hole 717c: the Bengal fan. Scientific Results 116, 155–161.

R Core Team, 2015. R: A Language and Environment for Statistical Computing. R Foundation for Statistical Computing, Vienna, Austria. https://www.r-project.org/.

Ravenscroft, P., Brammer, H., Richards, K., 2009. Arsenic Pollution - A Global Synthesis. Wiley-Blackwell, Chichester.

Redman, A.D., Macalady, D.L., Ahmann, D., 2002. Natural organic matter affects arsenic speciation and sorption onto hematite. Environmental Science and Technology 36, 2889–2896.

Reynolds, D.M., Ahmad, S.R., 1997. Rapid and direct determination of wastewater BOD values using a fluorescence technique. Water Research 31, 2012–2018.

Rhymes, J., Jones, L., Lapworth, D.J., White, D., Fenner, N., Mcdonald, J.E., Perkins, T.L., 2015. Using chemical, microbial and fluorescence techniques to understand contaminant sources and pathways to wetlands in a conversation site. The Science of the Total Environment 511, 703–710.

Richards, L.A., Casanueva-Marenco, M.J., Magnone, D., Sovann, C., van Dongen, B.E., Polya, D.A., 2019b. Contrasting sorption behaviours affecting groundwater arsenic concentraiton in Kandal Province, Cambodia. Geoscience Frontiers 10 (5), 1701–1713. https://doi.org/10.1016/j.gsf.2019.02.010.

Richards, L.A., Magnone, D., Boyce, A.J., Casanueva-Marenco, M.J., van Dongen, B.E., Ballentine, C.J., Polya, D.A., 2018. Delineating sources of groundwater recharge in an arsenic-affected Holocene aquifer in Cambodia using stable isotope-based mixing models. Journal of Hydrology 557, 321–334.

Richards, L.A., Magnone, D., Sovann, C., Kong, C., Uhlemann, S., Kuras, O., van Dongen, B.E., Ballentine, C.J., Polya, D.A., 2017a. High resolution profile of inorganic aqueous geochemistry and key redox zones in an arsenic bearing aquifer in Cambodia. The Science of the Total Environment 590 – 591, 540–553.

Richards, L.A., Magnone, D., Sültenfuß, J., Chambers, L., Bryant, C., Boyce, A.J., van Dongen, B.E., Ballentine, C.J., Sovann, C., Uhlemann, S., Kuras, O., Gooddy, D.C., Polya, D.A., 2019a. Dual in-aquifer and near surface processes drive arsenic mobilization in Cambodian groundwaters. The Science of the Total Environment 659, 699–714.

Richards, L.A., Magnone, D., van Dongen, B.E., Ballentine, C.J., Polya, D.A., 2015. Use of lithium tracers to quantify drilling fluid contamination for groundwater monitoring in Southeast Asia. Applied Geochemistry 63, 190–202.

Richards, L.A., Sültenfuß, J., Ballentine, C.J., Magnone, D., van Dongen, B.E., Sovann, C., Polya, D.A., 2017b. Tritium tracers of rapid surface water ingression into arsenic-bearing aquifers in the lower Mekong basin, Cambodia. Procedia Earth and Planetary Science 17, 845–848.

Rowland, H.A.L., Boothman, C., Pancost, R.D., Gault, A.G., Polya, D.A., Lloyd, J.R., 2009. The role of indigenous mircoorganisms in the biodegradation of naturally occurring petroleum, the reduction of iron, and the mobilization of arsenite from West Bengal aquifer sediments. Journal of Environmental Quality 38, 1598–1607.

Rowland, H.A.L., Gault, A.G., Lythgoe, P., Polya, D.A., 2008. Geochemistry of aquifer sediments and arsenic-rich groundwaters from Kandal Province, Cambodia. Applied Geochemistry 23, 3029–3046.

Rowland, H.A.L., Pederick, R.L., Polya, D.A., Pancost, R.D., van Dongen, B.E., Gault, A.G., Vaughan, D.J., Bryant, C., Anderson, B., Lloyd, J.R., 2007. The control of organic matter on microbially mediated iron reduction and arsenic release in shallow alluvial aquifers, Cambodia. Geobiology 5, 281–292.

Rowland, H.A.L., Polya, D.A., Lloyd, J.R., Pancost, R.D., 2006. Characterisation of organic matter in a shallow, reducing, arsenic-rich aquifer, West Bengal. Organic Geochemistry 37, 1101–1114.

Saadi, I., Borisover, M., Armon, R., Laor, Y., 2006. Monitoring of effluent DOM biodegradation using fluorescence, UV and DOC measurements. Chemosphere 63, 530–539.

Schittich, A.-R., Wünsch, U.J., Kulkarni, H.V., Battistel, M., Bregnhøj, H., Stedmon, C.A., McKnight, D., 2018. Investigating fluorescent organic-matter composition as a key predictor for arsenic mobility in groundwater aquifers. Environmental Science and Technology 52, 13027–13036.

Schoell, M., 1983. Genetic characterization of natural gases. The American Association of Petroleum Geologists Bulletin 67, 2225–2238.

Schoell, M., 1988. Multiple origins of methane in the Earth. Chemical Geology 71, 1–10.

Sengupta, S., McArthur, J., Sarkar, A., Leng, M.J., Ravenscroft, P., Howarth, R.J., Banerjee, D.M., 2008. Do ponds cause arsenic-pollution of groundwater in the Bengal Basin? An answer from West Bengal. Environmental Science and Technology 42, 5156–5164.

Sharma, P., Ofner, J., Kappler, A., 2010. Formation of binary and ternary colloids and dissolved complexes of organic matter, Fe and As. Environmental Science and Technology 44, 4479–4485.

Sharma, P., Rolle, M., Kocar, B., Fendorf, S., Kappler, A., 2011. Influence of natural organic matter on As transport and retention. Environmental Science and Technology 45, 546–553.

Sierra, M.M.D., Giovanela, M., Parlanti, E., Soriano-Sierra, E.J., 2005. Fluorescence fingerprint of fulvic and humic acids from varied origins as viewed by single-scan and excitation/emission matrix techniques. Chemosphere 58, 715–733.

Singh, S., D'sa, E., Swenson, E., 2010a. Seasonal variability in CDOM absorption and fluorescence properties in the Barataria Basin, Louisiana, USA. Journal of Environmental Sciences 22, 1481–1490.

Singh, S., D'sa, E.J., Swenson, E.M., 2010b. Chromophoric dissolved organic matter (CDOM) variability in Barataria Basin using excitation-emission matrix (EEM)

fluorescence and parallel factor analysis (PARAFAC). The Science of the Total Environment 408, 3211–3222.
Smedley, P.L., Kinniburgh, D.G., 2002. A review of the source, behaviour and distribution of arsenic in natural waters. Applied Geochemistry 17, 517–568.
Stedmon, C.A., Bro, R., 2008. Characterizing dissolved organic matter fluorescence with parallel factor analysis: a tutorial. Limnology and Oceanography: Methods 6.
Stedmon, C.A., Markager, S., Bro, R., 2003. Tracing dissolved organic matter in aquatic environments using a new approach to fluorescence spectroscopy. Marine Chemistry 82, 239–254.
Tamura, T., Saito, Y., Sieng, S., Ben, B., Kong, M., Choup, S., Tsukawaki, S., 2007. Depositional facies and radiocarbon ages of a drill core from the Mekong River lowland near Phnom Penh, Cambodia: evidence for tidal sedimentation at the time of Holocene maximum flooding. Journal of Asian Earth Sciences 29, 585–592.
Thurman, E., 1985. Organic Geochemistry of Natural Waters. Developments in Biogeochemistry. Junk Publishers, Boston, Ma.
Tye, A.M., Lapworth, D.J., 2016. Characterising changes in fluorescence properties of dissolved organic matter and links to N cycling in agricultural floodplains. Agriculture, Ecosystems & Environment 221, 245–257.
Uhlemann, S., Kuras, O., Richards, L.A., Naden, E., Polya, D.A., 2017. Electrical Resistivity Tomography determines the spatial distribution of clay layer thickness and aquifer vulnerability, Kandal Province, Cambodia. Journal of Asian Earth Sciences 147, 402–414.
van Dongen, B., Rowland, H.A.L., Gault, A.G., Polya, D.A., Bryant, C., Pancost, R.D., 2008. Hopane, sterane and n-alkane distributions in shallow sediments hosting high arsenic groundwaters in Cambodia. Applied Geochemistry 23, 3047–3058.
van Dongen, B.E., Talbot, H.M., Schouten, S., Pearson, P.N., Pancost, R.D., 2006. Well preserved palaeogene and cretaceous biomarkers from the Kilwa area, Tanzania. Organic Geochemistry 37, 539–557.
Vega, M.A., Kulkarni, H.V., Mladenov, N., Johannesson, K., Hettiarachchi, G.M., Bhattacharya, P., Kumar, N., Weeks, J., Galkaduwa, M., Datta, S., 2017. Biogeochemical controls on the release and accumulation of Mn and As in shallow aquifers, West Bengal, India. Frontiers in Environmental Science 5, 1–16.
Vonk, J.E., van Dongen, B.E., Gustafsson, Ö., 2008. Lipid biomarker investigation of the origin and diagenetic state of sub-arctic terrestrial organic matter presently exported into the northern Bothnian Bay. Marine Chemistry 112, 1–10.
Wang, C., Zhang, X., Wang, J., Chen, C., 2013. Characterization of dissolved organic matter as N-nitrosamine precursors based on hydrophobicity, molecular weight and fluorescence. Journal of Environmental Sciences 25, 85–95.
Wilson, H.F., Xenopoulos, M.A., 2009. Effects of Agricultural land use on the composition of fluvial dissolved organic matter. Nature Geoscience 2, 37–41.
Wolf, M., Kappler, A., Jiang, J., Meckenstock, R.U., 2009. Effects of humic substances and quinones at low concentrations on ferrihydrite reduction by *Geobacter metllireducens*. Environmental Science and Technology 43, 5679–5685.
World Health Organization, 2011. GuiDelines for Drinking-Water Quality, fourth ed. (Geneva).
Wu, J., Zhang, H., He, P.-J., Shao, L.-M., 2011. Insight into the heavy metal binding potential of dissolved organic matter in MSW leachate using EEM quenching combined with PARAFAC analysis. Water Research 45, 1711–1719.
Wu, J., Zhang, H., Shao, L.-M., He, P.-J., 2012a. Fluorescent characteristics and metal binding properties of individual molecular weight fractions in municipal solid waste leachate. Environmental Pollution 162, 63–71.
Wu, J., Zhang, H., Yao, Q.-S., Shao, L.-M., He, P.-J., 2012b. Toward understanding the role of individual fluorescent components in Dom-metal binding. Journal of Hazardous Materials 215 − 216, 294–301.
Zhang, T., Lu, J., Ma, J., Qiang, Z., 2008. Fluorescence spectroscopic characterization of DOM fractions isolated from a filtered river water after ozonation and catalytic ozonation. Chemosphere 71, 911–921.
Zou, X.M., Ruan, H.H., Fu, Y., Yang, X.D., Sha, L.Q., 2005. Estimating soil labile organic carbon and potential turnover rates using a sequential fumigation-incubation procedure. Soil Biology and Biochemistry 37, 1923–1928.
Zsolnay, A., Baiar, E., Jimenez, M., Steinweg, B., Saccomandi, F., 1999. Differentiating with fluorescence spectroscopy the sources of dissolved organic matter in soils subjected to drying. Chemosphere 38, 45–50.